

## Femtosecond pump-probe spectroscopy of polyatomic molecules in condensed phases

Yi Jing Yan and Shaul Mukamel

*Department of Chemistry, University of Rochester, Rochester, New York 14627*

(Received 30 November 1989)

A theory for ultrafast pump-probe spectroscopy of large polyatomic molecules in condensed phases is developed. A multimode Brownian oscillator model is used to account for high-frequency molecular vibrations and local intermolecular modes as well as collective solvent motions. A semi-classical picture is provided using the density matrix in Liouville space. The pump field creates a *doorway state* that propagates for a specified time interval, and the spectrum is calculated by finding its overlap with a *window state*, prepared by the probe pulse. The doorway and the window states are wave packets in phase space. For high-frequency modes and with long pulses they are expanded in the vibronic eigenstates, whereas for low-frequency modes and with impulsive pulses the Wigner (phase-space) representation is more adequate. Conditions for the observation of quantum beats, spectral diffusion, and solvation dynamics (dynamical Stokes shift) are specified.

### I. INTRODUCTION

Time-resolved optical measurements using picosecond or femtosecond pulses provide a novel probe for molecular nuclear motions and elementary photophysical and photochemical events. 100 fs laser pulses have been reported in 1981 and pulses as short as 6 fs are now being used.<sup>1</sup> Since the duration of such pulses is comparable to or shorter than typical molecular vibrational periods (the period of a  $330\text{-cm}^{-1}$  vibration is 100 fs), it becomes possible to observe molecular vibrations and other nuclear motions in real time. Nuclear motions on the femtosecond time scale have been observed in neat liquids,<sup>2-6</sup> in solids,<sup>7-9</sup> in solution,<sup>10-16</sup> in dye-doped polymer films,<sup>17</sup> and in isolated molecules in supersonic beams.<sup>18,19</sup> Molecular vibrations in condensed phases are subject to dissipative (friction) forces resulting from coupling to other intermolecular and intramolecular degrees of freedom. High-frequency vibrations undergo a coherent motion for many periods whereas low-frequency vibrations are usually overdamped and undergo diffusive (incoherent) motion. Coherent vibrations may show up in femtosecond spectroscopy as quantum beats. Quantum beats constitute the simplest example of quantum-mechanical interference. When two levels are excited coherently and emit to a common final level, the emission spectrum oscillates with the two-level frequency. Microsecond to nanosecond quantum beats are well known in atomic Zeeman spectroscopy.<sup>20</sup> It has been demonstrated that using a femtosecond excitation one can readily observe beats in very large dye molecules at room temperature and in condensed phases. The techniques most commonly used are the impulsive-stimulated light scattering,<sup>2,4,5,7-9</sup> pump-probe absorption,<sup>3,6,10-17</sup> and time-resolved fluorescence.<sup>18,21</sup>

In the impulsive scattering technique two laser pulses with wave vectors  $\mathbf{k}_1$  and  $\mathbf{k}_2$  interact simultaneously with the sample, creating a transient grating with a wave vector  $\mathbf{k}_1 - \mathbf{k}_2$ . After a delay time  $\tau$ , a third pulse with wave

vector  $\mathbf{k}_1$  is scattered from the sample, and the signal with wave vector  $2\mathbf{k}_1 - \mathbf{k}_2$  is detected. The laser pulses are usually tuned way off resonance from any optical transition and the signal is then related to the Fourier transform of the spontaneous Raman experiment. Nelson and co-workers first applied the impulsive stimulated emission technique to study acoustic phonons in glasses on the picosecond time scale.<sup>7</sup> Subsequent femtosecond studies were then performed on a variety of systems, including optical phonons in molecular crystals,<sup>8</sup> and intramolecular,<sup>3</sup> orientational, and intermolecular<sup>4</sup> motions in molecular liquids. Coherent vibrational motion in liquid  $\text{CH}_2\text{Br}_2$  was observed by Ruhman, Joly, and Nelson<sup>3</sup> using a two-pulse off-resonant experiment. The transmitted probe intensity shows a  $173\text{-cm}^{-1}$  oscillation corresponding to a bending mode fundamental. This reflects a periodic spectral shift in the transmitted probe field as the delay time  $\tau$  is varied. Therefore the phase of the beats depends strongly on the optical frequency of observation. More recently it has been shown that multiple femtosecond pulse sequences may improve the mode selectivity of these experiments.<sup>22</sup>

The first terahertz oscillations in saturated resonant absorption using two pulses was observed by Tang and co-workers in malachite green (MG) and several other triphenyl methane dyes in solution using 40-fs optical pulses.<sup>11</sup> The combined transmitted intensity of the pump and the probe is measured as a function of the pulse delay time  $\tau$ . The same group further measured the frequency dispersed signals of ethyl violet in solution.<sup>12</sup> In contrast to the off-resonance case, the phase of this quantum beat signal does not vary substantially with the dispersed frequency. Fragnito *et al.* reported recently the probe absorption of MG in solution using 6-fs optical pulses, showing coherent vibrational motions in the  $1200\text{--}1600\text{-cm}^{-1}$  frequency range.<sup>16</sup> Chesnoy and Mokhtari performed a variety of polarization-sensitive resonant probe absorption measurements on MG in solution.<sup>13</sup> These techniques allow the separate measurement

of the absorptive and the dispersive contributions to the molecular polarization induced by the excitation pulses. Excited-state and ground-state molecular dynamics were then resolved.

The vibrational quantum beats observed in all of these experiments contain simple damped harmonic oscillations with periods of only a few molecular vibrations. These observations raise many interesting questions such as the following: How does the experiment select a single vibrational mode? Do the beats represent ground-state or excited-state evolution? What is the role of coupling to the medium (homogeneous, inhomogeneous broadening, and spectral diffusion processes) in these measurements? Nelson and co-workers<sup>23,24</sup> interpreted their off-resonant impulsive stimulated experiments with a phenomenological model based on a damped and impulsively driven harmonic oscillator evolving in the ground electronic state. The driving force is induced by the impulsive coupling of the molecular transition dipole and the pump pulse. The probe field then interacts with the driven oscillator in and out of phase periodically. If they are in phase, the probe field will lose energy to the medium (red shift), while if they are out of phase, it will gain energy from the medium (blue shift). The role of the solvent is described, in this model, by a frictional damping constant. The driven oscillator model does not apply for the interpretation of impulsive resonant experiments where excitation processes create a significant population in the electronic excited state and the molecular dynamics in both the electronic ground and excited potential surfaces may be important. Stock and Domeke<sup>25</sup> and Fragnito *et al.*<sup>16</sup> interpreted the excited-state vibrational dynamics as a coherent motion of a nuclear wave packet in the electronic excited state. The coupling to the solvent motion may not be included in this wave-function formalism. Theoretical treatments which apply to both the resonant and the off-resonant experiments were made by using the Bloch equation for the density matrix.<sup>12,13,26,27</sup> These treatments use up to four vibronic levels (two in the ground state and two in the excited state). The solvation dynamics are incorporated through homogeneous broadening (electronic dephasing), inhomogeneous broadening, and the vibrational dephasing processes.

In this paper we present a unified theory of time-resolved pump-probe spectroscopy using a microscopic correlation function approach.<sup>28</sup> The molecular dynamics is calculated in Liouville (phase) space using the Wigner representation for nuclear motions.<sup>29,30</sup> For the sake of clarity we consider an ideal situation in which the pump and the probe are well separated in time. This allows us to ignore the coherent artifact which complicates the interpretation (although it can be included if necessary).<sup>31</sup> The rate of solvent relaxation, compared to the pulse durations, can either be very short, resulting in pure electronic dephasing processes (homogeneous broadening); intermediate, showing spectral diffusion processes; or very long, resulting in the inhomogeneous broadening. The following picture for pump-probe spectroscopy is developed in this article: We consider the relevant phase space of the system. This can consist of the relevant vibrations, solvent modes, etc. The pump

pulse interacts with the system and creates a nonequilibrium density matrix which then evolves in time for a period  $\tau$  (the delay between the pump and the probe). This density matrix is called the *doorway function*. We further need to define a *window function*. This is a phase-space distribution which the probe pulse is monitoring. The probe absorption is calculated by evaluating the phase-space overlap of the doorway and the window functions. The main advantages of the present theory are as follows. First, it is valid both for resonant and off-resonant experiments. Second, it allows the incorporation of solvation dynamics with arbitrary time scales [including spectral diffusion processes, which are responsible for the spectral (Stokes) shifts,<sup>32–36</sup> homogeneous, and inhomogeneous broadening processes]. Third, the molecular dynamics are formulated in phase space and can be easily evaluated semiclassically. This way we avoid the tedious multiple summations over eigenstates which restrict the usage of eigenstate based expressions to small systems. Finally, the present results, which are based on the nonlinear response function, can be directly applied to other related nonlinear spectroscopies.<sup>28–30</sup> The present theory provides a transparent physical picture of time-resolved pump-probe experiments and is valid for an arbitrary excitation pulse duration. In the impulsive pump limit, in which the duration of the pump pulse is much shorter than the molecular dynamics, the coherent vibronic motion in phase space is monitored.<sup>37</sup> The present theory, in this case, recovers the wave-packet results.<sup>16,25</sup> Moreover, in the off-resonant configuration, the present theory reduces to the driven oscillator model.<sup>23,24</sup> When the pulse duration is short and comparable to the nuclear dynamics, only a few vibronic levels are coherently excited, and the present theory recovers the earlier treatments of quantum beats using the vibronic level representation.<sup>12,13,26,27</sup> In the other limit, where the pump duration is long compared to the nuclear motions of the chromophore but short compared to the solvent reorganization processes, the present formalism recovers the theory of time-resolved hole burning.<sup>36</sup> In this case, only the diffusive solvation dynamics as well as the vibronic populations of the chromophore are probed. The present formalism applies also to femtosecond spectroscopy in isolated molecules in supersonic beams where bond breaking, nonadiabatic transitions, and quantum beats have recently been reported.<sup>38–40</sup> It also offers an insight on recent schemes suggested to achieve laser control of molecular reactions.<sup>41</sup>

The remainder of the paper is organized as follows. In Sec. II we develop the basic formal expressions of the nonlinear optical polarization  $P^{(3)}$  and for probe absorption using the doorway and the window functions. The doorway function depends on the pump pulse shape whereas the window function depends on the probe pulse shape. In Sec. III we consider a simplified limiting case in which the doorway and the window functions depend only on the pulse frequencies but not on their temporal profiles. The resulting *bare spectrum* is a useful concept. Under very general conditions the observed spectrum may be calculated by convoluting the bare spectrum with either the temporal or the spectral intensity profiles of the

incoming pulses. Formal expressions for the bare doorway and the bare window functions using the vibronic state representation are given. In Sec. IV, the optical signal is further represented in the Wigner phase space and the molecular dynamics are calculated via the generalized Langevin equations using a multimode Brownian oscillator model. In Sec. V we focus on the contribution of low-frequency modes and solvation dynamics by considering strongly overdamped (diffusive) nuclear motions. These coordinates may describe dielectric relaxation, spectral diffusion, as well as the homogeneous and the inhomogeneous broadening, depending on the magnitude of their characteristic time scales and their coupling strength to the electronic transition. In Sec. VI, we consider impulsive spectroscopy and examine the coherent vibrational motion in phase space. The effect of the solvation dynamics on the beats signal is analyzed. We further consider off-resonant impulsive spectroscopy where non-Condon effects play an essential role. Finally, in Sec. VII, we present general expressions for the probe absorption signal which hold for arbitrary pulse durations. Optical selectivity controlled by the pump pulse duration is discussed. As the pulsed duration increases, the experiment varies from the impulsive configuration to the hole burning configuration.

## II. DOORWAY-WINDOW PICTURE OF PUMP-PROBE SPECTROSCOPY

We consider a molecular system interacting with an external electromagnetic field  $E(\mathbf{r}, t)$ . The total Hamiltonian of the system in the dipole approximation is

$$H_T = H - VE(\mathbf{r}, t) . \quad (2.1)$$

Here  $H$  is the molecular Hamiltonian in the absence of the external field. The second term in Eq. (2.1) represents the molecule-field dipolar interaction with  $V$  being the molecular dipole operator. We shall consider  $V$  and  $E$  to be scalar quantities. Their vector nature is important when studying orientational effects which can be detected by varying the polarization of the light fields.<sup>6,13</sup> These effects will not be considered in this article. In a pump-probe experiment the system is subjected to two light pulses: the pump pulse whose frequency is centered around  $\Omega_1$ , and the probe pulse whose frequency is centered around  $\Omega_2$ . The external field is then given by

$$\begin{aligned} E(\mathbf{r}, t) = & E_1(t + \tau) \exp(i\mathbf{k}_1 \cdot \mathbf{r} - i\Omega_1 t) \\ & + E_1^*(t + \tau) \exp(-i\mathbf{k}_1 \cdot \mathbf{r} + i\Omega_1 t) \\ & + E_2(t) \exp(i\mathbf{k}_2 \cdot \mathbf{r} - i\Omega_2 t) \\ & + E_2^*(t) \exp(-i\mathbf{k}_2 \cdot \mathbf{r} + i\Omega_2 t) . \end{aligned} \quad (2.2)$$

Here  $E_1(t + \tau)$  and  $E_2(t)$  are the temporal envelopes of the pump field and the probe field, respectively. The asterisk represents the complex conjugate. We shall further introduce the Fourier transform of the optical pulse envelopes:

$$\hat{E}_j(\omega_j) = (2\pi)^{-1/2} \int_{-\infty}^{\infty} dt \exp[i(\omega_j - \Omega_j)t] E_j(t) , \quad j=1,2 . \quad (2.3)$$

We assume that the pump pulse is peaked at time  $t = -\tau$ , while the probe pulse is peaked at  $t = 0$ . The time delay  $\tau$  of the probe pulse with respect to the pump pulse can be continuously varied, allowing the probe to interact with the system either before ( $\tau < 0$ ) or after ( $\tau > 0$ ) the pump field.

In this paper we shall calculate the probe difference absorption, defined as the total probe absorption in the presence of pump minus the probe absorption in the absence of the pump.<sup>3,13-17,41</sup> The probe absorption is commonly detected using one of the following two schemes. In the first scheme the total integrated intensity<sup>6,11,13,17,41</sup> of the transmitted probe field is measured and the integrated signal  $S(\Omega_1, \Omega_2; \tau)$  is obtained as the function of the delay time  $\tau$  and  $\Omega_2$ , the center frequency of the probe field. We then have<sup>40</sup>

$$\begin{aligned} S(\Omega_1, \Omega_2; \tau) = & -2 \operatorname{Im} \int_{-\infty}^{\infty} dt E_2^*(t) P^{(3)}(\mathbf{k}_2, t) \\ \equiv & \int_{-\infty}^{\infty} d\omega_2 S'(\Omega_1, \Omega_2; \omega_2, \tau) , \end{aligned} \quad (2.4a)$$

Here,  $P^{(3)}(\mathbf{k}_2, t)$  represents the polarization in the optical medium, induced by the third-order interaction with the external field<sup>28</sup> with wave vector  $\mathbf{k}_2 = -\mathbf{k}_1 + \mathbf{k}_1 + \mathbf{k}_2$ . It should be noted that this is the same polarization which is probed in the impulsive-stimulated light-scattering experiments with a three pulse excitation schemes.<sup>23,28</sup> In Eq. (2.4a),  $S'(\Omega_1, \Omega_2; \omega_2, \tau)$  represents the differential signal obtained by the second detection scheme, in which the transmitted probe field is dispersed through a monochromator and the signal is measured as a function of the dispersed frequency  $\omega_2$ .<sup>3,12,14-16</sup> The formal expression for  $S'$  may be obtained by solving the Maxwell equation using the polarization field  $P^{(3)}$  as a source.<sup>36,42</sup> It can also be derived by performing a Fourier transform of Eq. (2.4a) resulting in

$$S'(\Omega_1, \Omega_2; \omega_2, \tau) = -2 \operatorname{Im} \hat{E}_2^*(\omega_2) \hat{P}^{(3)}(\omega_2) . \quad (2.4b)$$

Here  $\hat{E}_2(\omega_2)$  is the probe field amplitude [Eq. (2.3)], and  $\hat{P}^{(3)}(\omega_2)$  is the  $\omega_2$  Fourier component of the third-order polarization,

$$\hat{P}^{(3)}(\omega_2) = (2\pi)^{-1/2} \int_{-\infty}^{\infty} dt \exp[i(\omega_2 - \Omega_2)t] P^{(3)}(\mathbf{k}_2, t) . \quad (2.5)$$

Hereafter we shall consider only the integrated signal [Eq. (2.4a)]. The calculation of Eq. (2.4b) is straightforward using the quantities derived in this article.

Equation (2.4) is general and is valid for an arbitrary molecular system. We shall now specify our molecular system and consider a polyatomic molecule with two electronic states, embedded in a solvent. The material Hamiltonian and the electronic transition dipole in Eq. (2.1) assume the form

$$H = |g\rangle H_g \langle g| + |e\rangle H_e \langle e| , \quad (2.6a)$$

$$V = \mu(|g\rangle \langle e| + |e\rangle \langle g|) . \quad (2.6b)$$

Here  $H_g$  and  $H_e$  are the adiabatic nuclear Hamiltonians of the molecule and the solvent in the ground and in the excited electronic states, respectively.  $\mu$  is the electronic matrix element of the dipole operator which depends on the nuclear coordinates. We shall further assume that initially the system is in thermal equilibrium in its ground electronic state, i.e.,

$$\rho(-\infty) = |g\rangle\rho_g\langle g|. \quad (2.7)$$

Here  $\rho_g$  is the equilibrium nuclear density matrix in the ground state. We further introduce the Liouville space Green's function  $\mathcal{G}_{mm}(t)$  defined by its action on an arbitrary dynamical variable  $A$ ,

$$\mathcal{G}_{mm}(t)A = \exp(-iH_m t)A \exp(iH_m t), \quad m = g, e. \quad (2.8)$$

In this paper we shall calculate the probe absorption [Eq. (2.4)] when the probe field is well separated from the pump field (i.e., the duration of both pulses is much shorter than their relative delay time  $\tau$ ). This condition implies that the system first interacts with the pump field and then with the probe field. In the Appendix we calculate the probe absorption signal [Eq. (2.4a)]. Within the rotating-wave approximation, the resulting spectrum is

$$S(\Omega_1, \Omega_2; \tau) = \text{Tr}[\hat{W}_e(\Omega_2)\mathcal{G}_{ee}(\tau)\hat{D}_e(\Omega_1)] \\ + \text{Tr}[\hat{W}_g(\Omega_2)\mathcal{G}_{gg}(\tau)\hat{D}_g(\Omega_1)], \quad (2.9)$$

where

$$\hat{D}_e(\Omega_1) = \int_{-\infty}^{\infty} dt' \int_0^{\infty} dt_1 E_1^*(t')E_1(t'-t_1)\exp(i\Omega_1 t_1) \\ \times [\exp(iH_e t')\exp(-iH_e t_1)\mu\rho_g \\ \times \exp(iH_g t_1)\mu \exp(-iH_e t')] + \text{H.c.} \quad (2.10a)$$

$$\hat{D}_g(\Omega_1) = \int_{-\infty}^{\infty} dt' \int_0^{\infty} dt_1 E_1^*(t')E_1(t'-t_1)\exp(i\Omega_1 t_1) \\ \times [\exp(iH_g t')\mu \exp(-iH_e t_1)\mu\rho_g \\ \times \exp(iH_g t_1)\exp(-iH_g t')] + \text{H.c.}, \quad (2.10b)$$

$$\hat{W}_e(\Omega_2) = \int_{-\infty}^{\infty} dt \int_0^{\infty} dt_3 E_2^*(t+t_3)E_2(t)\exp(i\Omega_2 t_3) \\ \times [\exp(iH_e t)\mu \exp(iH_g t_3)\mu \\ \times \exp(-iH_e t_3)\exp(-iH_e t)] \\ + \text{H.c.}, \quad (2.11a)$$

$$\hat{W}_g(\Omega_2) = \int_{-\infty}^{\infty} dt \int_0^{\infty} dt_3 E_2^*(t+t_3)E_2(t)\exp(i\Omega_2 t_3) \\ \times [\exp(iH_g t)\exp(iH_g t_3)\mu \\ \times \exp(-iH_e t_3)\mu \exp(-iH_g t)] \\ + \text{H.c.}, \quad (2.11b)$$

Here H.c. denotes the Hermitian conjugate. Two-sided Feynman diagrams representing the probe absorption [Eq. (2.9)] are given in Fig. 1.

Equation (2.9) provides the following physical picture of the pump probe experiment. The pump field transfers a fraction of the molecules from the ground state to the excited state, creating a "particle" in the excited electronic state, and a "hole" in the ground electronic state. The density matrix representing the particle and the hole is given by doorway operators  $\hat{D}_e$  and  $\hat{D}_g$ , respectively. Similarly, the probe field creates the window operators,  $\hat{W}_e$  for the particle and  $\hat{W}_g$  for the hole. All the operators  $\hat{D}_e$ ,  $\hat{D}_g$ ,  $\hat{W}_g$ , and  $\hat{W}_e$  are Hermitian. The first term in Eq. (2.9) represents the particle contribution to the probe absorption which is simply given by the overlap of the particle doorway, propagated for the delay time  $\tau$ , with the particle window. The propagation takes place on the excited potential surface and is represented by  $\mathcal{G}_{ee}(\tau)$ . The hole makes a similar contribution with its own doorway and window operators and with the propagation taking place on the ground-state surface, as given by  $\mathcal{G}_{gg}(\tau)$ . This contribution is the second term in Eq. (2.9). Note that the doorway operators [Eq. (2.10)] contain the equilibrium density matrix  $\rho_g$  whereas the window operators [Eq. (2.11)] can be obtained from the doorway operators by interchanging the fields  $E_1$  and  $E_2$  and by replacing the ground-state density matrix  $\rho_g$  with the unit operator. In that respect the window operators correspond the infinite temperature limit of the doorway operators.<sup>40</sup>

The frequency dispersed detection scheme [Eq. (2.4b)] leads to an expression similar to Eq. (2.9) with the window operators  $\hat{W}_e(\Omega_2)$  and  $\hat{W}_g(\Omega_2)$  replaced by  $\hat{W}'_e(\Omega_2; \omega_2)$  and  $\hat{W}'_g(\Omega_2; \omega_2)$ , respectively,

$$\hat{W}'_e(\Omega_2; \omega_2) = (2\pi)^{-1/2} E_2^*(\omega_2) \int_{-\infty}^{\infty} dt \int_0^{\infty} dt_3 E_2(t)\exp[i(\omega_2 - \Omega_2)t]\exp(i\omega_2 t_3) \\ \times [\exp(iH_e t)\mu \exp(iH_g t_3)\mu \exp(-iH_e t_3)\exp(-iH_e t)] + \text{H.c.}, \quad (2.12a)$$

$$\hat{W}'_g(\Omega_2; \omega_2) = (2\pi)^{-1/2} E_2^*(\omega_2) \int_{-\infty}^{\infty} dt \int_0^{\infty} dt_3 E_2(t)\exp[i(\omega_2 - \Omega_2)t]\exp(i\omega_2 t_3) \\ \times [\exp(iH_g t)\exp(iH_g t_3)\mu \exp(-iH_e t_3)\mu \exp(-iH_g t)] + \text{H.c.} \quad (2.12b)$$

We shall not consider this detection scheme any further in this article.

Equations (2.9)–(2.11) constitute our final formal doorway-window picture of pump-probe spectroscopy. In this picture the fourfold temporal integrations implied in Eqs. (2.4), (2.5), and Eq. (A1) are factorized into a two-

fold integration for the doorway function and a twofold integration for the window function. We reiterate that the only approximations made in the derivation of Eqs. (2.9)–(2.11) are the assumption that the pulses are well separated in time and the rotating-wave approximation. The off-resonant terms neglected in the rotating-wave ap-

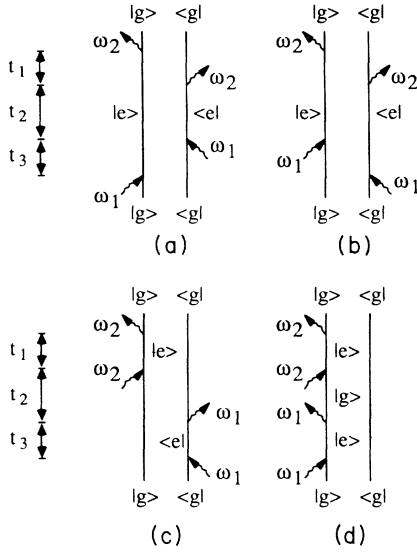


FIG. 1. Four double-sided Feynman diagrams representing the probe difference absorption [Eq. (2.9)] in the rotating-wave approximation (Refs. 40 and 42). The left and the right vertical lines represent the ket and the bra of the density matrix, respectively, and the time runs from bottom to top. The wavy arrow represents a matter-field interaction. The complex conjugate contribution can be obtained by exchanging the ket and the bra. Diagrams (a) and (b) together with their complex conjugates represent the “particle” dynamics in the excited electronic state [the first term of Eq. (2.9)], whereas diagrams (c) and (d) together with their complex conjugates represent the “hole” dynamics in the ground electronic state [the second term of Eq. (2.9)].  $t_1$ ,  $t_2$ , and  $t_3$  represent the time intervals between the successive matter-field interactions. The relevant time scale of  $t_1$  and  $t_3$  is controlled by the electronic dephasing, and  $t_2 = \tau + t - t'$ . Here,  $\tau$  is the delay time.  $t_1$  and  $t'$  are bounded by pump duration [cf. Eq. (2.10)], while  $t_3$  and  $t$  by probe duration [cf. Eq. (2.11)].

proximation may be important in impulsive experiments or for off-resonant excitation. In this case, we should use the more general expressions [Eqs. (A7)] for the doorway and window which contain three additional terms to Eqs. (2.10) and (2.11). Equations (2.9)–(2.11) will further be simplified in the following section by considering special conditions which usually hold in current pump-probe experiments.

### III. PROBE ABSORPTION: VIBRONIC STATE REPRESENTATION

In this section we consider some typical experimental situations in which the calculation of the probe absorption is considerably simplified.

#### A. Bare spectrum:

##### Pulses short compared with nuclear dynamics and long compared with electronic dephasing

The final expression for the spectrum [Eqs. (2.9)–(2.11)] has four time integrations. As illustrated in Fig. 1, dur-

ing the time periods  $t_1$  and  $t_3$  the system is in an *optical coherence* ( $\rho_{eg}$  or  $\rho_{ge}$ ) whereas during the time periods  $t$ ,  $t'$ , and  $\tau$  is in a population ( $\rho_{ee}$  or  $\rho_{gg}$ ). The relevant magnitude of these time scales depends on the laser pulse duration ( $E_1$  controls  $t_1$  and  $t'$ ,  $E_2$  controls  $t_3$  and  $t$ ) as well as on the relevant dynamics of the system being probed. Let us ignore for a moment the pulse influence and concentrate on the molecular system. The time evolution of the coherence includes a time-dependent phase arising from the nuclear degrees of freedom. This phase depends on the initial configuration of the nuclei. When an ensemble average is performed over these initial conditions it results in an irreversible fast decay known as *pure dephasing*.<sup>28</sup> Consequently, the time scales  $t_1$  and  $t_3$  are dominated by the pure dephasing processes and are very short. During the  $\tau$ ,  $t$ , and  $t'$  periods the system is in an electronic population ( $\rho_{ee}$  for the particle and  $\rho_{gg}$  for the hole). The relevant time scale of nuclear motion is typically much longer than the dephasing time scale. The simplified picture given below holds when the dephasing time scale is much shorter than the molecular dynamics, and the pulse durations are adjusted to be intermediate between these two times scales. We then obtain the *bare spectrum*, which describes an ideal situation in which the pulses can be considered both monochromatic (with respect to the relevant linewidth related to the inverse dephasing timescale) and infinitely short (with respect to the molecular nuclear dynamics).<sup>40</sup> Using the conditions specific above, we make the following two approximations.

(i) Since the pulses are short compared with molecular nuclear dynamics, we may neglect the molecular dynamics during the time  $t'$  and  $t$  periods in the integrands of Eqs. (2.10) and (2.11) by approximating

$$\exp(\pm iH_m t') \approx \exp(\pm iH_m t) \approx 1, \quad m = g, e. \quad (3.1)$$

(ii) Since the dephasing time scale is much shorter than the pulse durations, we can neglect the variation of the external pulses on the  $t$  and  $t_3$  time scales, resulting in<sup>40</sup>

$$E_1^*(t')E_1(t'-t_1) \approx |E_1(t')|^2, \quad (3.2a)$$

$$E_2^*(t+t_3)E_2(t) \approx |E_2(t)|^2. \quad (3.2b)$$

When approximations (i) and (ii) are introduced in Eqs. (2.10) and (2.11), the spectrum [Eq. (2.9)] becomes (up to a proportionality factor)

$$S_0(\Omega_1\Omega_2; \tau) \equiv \text{Tr}[\hat{W}_e^0(\Omega_2)\mathcal{G}_{ee}(\tau)\hat{D}_e^0(\Omega_1)] \\ + \text{Tr}[\hat{W}_g^0(\Omega_2)\mathcal{G}_{gg}(\tau)\hat{D}_g^0(\Omega_1)], \quad (3.3)$$

with

$$\hat{D}_e^0(\Omega_1) \equiv \int_0^\infty dt_1 \exp(i\Omega_1 t_1) \\ \times [\exp(-iH_e t_1)\mu\rho_g \exp(iH_g t_1)\mu] + \text{H.c.}, \quad (3.4a)$$

$$\hat{D}_g^0(\Omega_1) \equiv \int_0^\infty dt_1 \exp(i\Omega_1 t_1) \\ \times [\mu \exp(-iH_e t_1)\mu\rho_g \exp(iH_g t_1)] + \text{H.c.}, \quad (3.4b)$$

$$\hat{W}_e^0(\Omega_2) \equiv \int_0^\infty dt_3 \exp(i\Omega_2 t_3) \times [\mu \exp(iH_g t_3) \mu \exp(-iH_e t_3)] + \text{H.c.}, \quad (3.5a)$$

$$\hat{W}_g^0(\Omega_2) \equiv \int_0^\infty dt_3 \exp(i\Omega_2 t_3) \times [\exp(iH_g t_3) \mu \exp(-iH_e t_3) \mu] + \text{H.c.} \quad (3.5b)$$

We shall denote  $S_0$  the *bare spectrum*. The name implies that the spectrum does not depend on the light pulse shapes and is an intrinsic molecular property (although proper light pulses are essential in order to observe the bare spectrum). Equations (3.4) and (3.5) define the *bare doorway* and the *bare window* operators, respectively. They are considerably simpler than their counterparts [Eqs. (2.10) and (2.11)] since each contains a single (rather than a double) time integration. In addition, they do not depend on the light pulse shapes, but only on their frequencies  $\Omega_1$  and  $\Omega_2$ .

In order to get a better feeling for the bare doorway and window operators we shall expand them in a complete basis set of the molecular vibronic eigenstates. We denote the eigenstates of  $H_g$  by  $a, c, \dots$ , and  $H_e$  by  $b, d, \dots$ , i.e.,

$$\begin{aligned} H_g |v\rangle &= \varepsilon_v |v\rangle, \quad v = a, c, \dots, \\ H_e |v\rangle &= \varepsilon_v |v\rangle, \quad v = b, d, \dots \end{aligned} \quad (3.6)$$

We shall further denote the 0-0 electronic transition frequency as  $\omega_{eg}$  (see Fig. 2). Using this basis set, we have

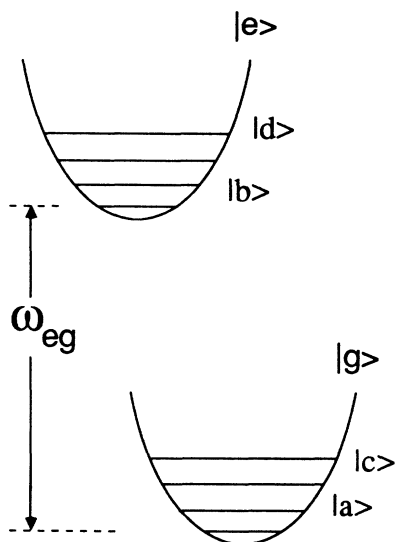


FIG. 2. The molecular vibronic level scheme introduced in Eqs. (2.6) and (3.6).  $|a\rangle$  and  $|c\rangle$  are vibronic levels corresponding to the ground electronic manifold  $|g\rangle$ .  $|b\rangle$  and  $|d\rangle$  are vibronic levels corresponding to the excited electronic manifold  $|e\rangle$ .  $\omega_{eg}$  is the 0-0 electronic transition frequency.

$$\hat{D}_e^0(\Omega_1) = i \sum_{d,b} |d\rangle \langle b| \left[ \sum_a P(a) \mu_{da} \mu_{ab} \times \left[ \frac{1}{\Omega_1 - \omega_{da} + i\gamma/2} - \frac{1}{\Omega_1 - \omega_{ba} - i\gamma/2} \right] \right], \quad (3.7a)$$

$$\hat{D}_g^0(\Omega_1) = i \sum_{c,a} |c\rangle \langle a| \left[ \sum_d \mu_{cd} \mu_{da} \times \left[ \frac{P(a)}{\Omega_1 - \omega_{da} + i\gamma/2} - \frac{P(c)}{\Omega_1 - \omega_{dc} - i\gamma/2} \right] \right], \quad (3.7b)$$

$$\hat{W}_e^0(\Omega_2) = i \sum_{d,b} |d\rangle \langle b| \left[ \sum_c \mu_{dc} \mu_{cb} \times \left[ \frac{1}{\Omega_2 - \omega_{bc} + i\gamma/2} - \frac{1}{\Omega_2 - \omega_{dc} - i\gamma/2} \right] \right], \quad (3.8a)$$

$$\hat{W}_g^0(\Omega_2) = i \sum_{c,a} |c\rangle \langle a| \left[ \sum_b \mu_{cb} \mu_{ba} \times \left[ \frac{1}{\Omega_2 - \omega_{bc} + i\gamma/2} - \frac{1}{\Omega_2 - \omega_{ba} - i\gamma/2} \right] \right]. \quad (3.8b)$$

Here  $\hbar\omega_{vv'} \equiv \varepsilon_v - \varepsilon_{v'}$  is the energy difference between the vibronic levels  $v$  and  $v'$ .  $P(v)$  is the thermal equilibrium population of the  $v$ th vibronic level.  $\gamma$  is the inverse lifetime of the excited electronic state.

When the pump excitation is tuned far off resonance from the electronic transition, we expect the particle contribution to the spectrum to vanish and the signal should reflect solely the hole dynamics in the ground state.<sup>28</sup> In order to see how this limit is obtained we shall examine the asymptotic behavior of the doorway states following an off-resonance pump excitation, in which the detuning  $|\Omega_1 - \omega_{eg}|$  is much larger than the vibronic level spacings in the same electronic state,  $\omega_{db}$  or  $\omega_{ca}$ , and Eqs. (3.7) reduce to

$$\hat{D}_e^0(\Omega_1) \approx \sum_{d,b} |d\rangle \langle b| \left[ \sum_a P(a) \mu_{da} \mu_{ab} \frac{\gamma}{(\Omega_1 - \omega_{eg})^2} \right], \quad (3.9a)$$

$$\hat{D}_g^0(\Omega_1) \approx \sum_{c,a} |c\rangle \langle a| \left[ \sum_d \mu_{cd} \mu_{da} \left[ \frac{\gamma}{2} \frac{P(a)+P(c)}{(\Omega_1 - \omega_{eg})^2} + i \frac{P(a)-P(c)}{\Omega_1 - \omega_{eg}} \right] \right],$$

$$|\Omega_1 - \omega_{eg}| \gg \omega_{\nu\nu'}. \quad (3.9b)$$

Both the excited-state doorway and the ground-state doorway contain a real contribution that varies as  $\gamma/(\Omega_1 - \omega_{eg})^2$ . The ground doorway contains in addition an imaginary contribution that varies as  $1/(\Omega_1 - \omega_{eg})$ . For large detunings the real part vanishes much more rapidly than the imaginary part not only due to the larger power  $[(\Omega_1 - \omega_{eg})^{-2}$  versus  $(\Omega_1 - \omega_{eg})^{-1}]$ , but also since the damping constant  $\gamma$  is usually frequency dependent  $\gamma(\Omega_1)$  and it always vanishes for large off-resonance detunings.<sup>28</sup> Consequently, the excited-state (particle) doorway state can be neglected for off-resonance excitation and we need consider only the ground-state (hole) doorway whose contribution is purely imaginary. It is interesting to note that the vanishing of the real part is a result of an interference between two Liouville space pathways. It is the same interference that leads to the absence of excited-state frequencies in coherent anti-Stokes

Raman (CARS) spectroscopy of isolated molecules. When dephasing is added, the interference is no longer fully destructive, which gives rise to dephasing-induced extra-narrow resonances.<sup>28(c)</sup>

In concluding this section, we shall consider the *classical limit*,<sup>43,44</sup> where we assume that the optical transition occurs instantaneously, and further, the transition dipole does not depend on the nuclear coordinates  $\mu(Q) = \mu_{eg}$  (the Condon approximation). It is better in this case to use the formal expressions [Eqs. (3.4) and (3.5)] rather than the eigenstate expansion. Neglecting commutations in these equations we write (for  $t = t_1$  and  $t_3$ )

$$\exp(-iH_e t) \exp(iH_g t) \cong \exp(-iUt), \quad (3.10a)$$

with

$$U \equiv H_e - H_g \quad (3.10b)$$

as the potential energy difference between the two electronic surfaces. Upon the substitution of Eq. (3.10) in Eqs. (3.3)–(3.5), we get

$$\hat{D}_e^0(\Omega_1) = \hat{D}_g^0(\Omega_1) = 2\pi |\mu_{eg}|^2 \delta(\Omega_1 - U) \rho_g, \quad (3.11a)$$

$$\hat{W}_e^0(\Omega_2) = \hat{W}_g^0(\Omega_2) = 2\pi |\mu_{eg}|^2 \delta(\Omega_2 - U), \quad (3.11b)$$

and

$$S_0(\Omega_1, \Omega_2; \tau) = 4\pi^2 |\mu_{eg}|^4 \text{Tr} \{ \delta(\Omega_2 - U) [\exp(-iH_e \tau) \delta(\Omega_1 - U) \rho_g \exp(iH_e \tau)] \}$$

$$+ 4\pi^2 |\mu_{eg}|^4 \text{Tr} \{ \delta(\Omega_2 - U) [\exp(-iH_g \tau) \delta(\Omega_1 - U) \rho_g \exp(iH_g \tau)] \}. \quad (3.12)$$

This result has a simple classical interpretation, related to the classical Condon approximation,<sup>43,44</sup> which states that a photon  $\Omega$  can be absorbed or emitted only in nuclear configurations with  $U = \Omega$ . Let us consider the first term in Eq. (3.12). The initial doorway state is  $\sim \delta(\Omega_1 - U) \rho_g$ . Its subsequent evolution for the delay period  $\tau$  is governed by the excited-state Hamiltonian  $H_e$ . This leads to the term in the square brackets. The probe pulse creates a window function  $\delta(\Omega_2 - U)$ . The particle contribution to the spectrum is given by the overlap of the propagated doorway function with the window function. The second term in Eq. (3.12) can be interpreted similarly except that the propagation during the  $\tau$  period is given by the ground-state Hamiltonian  $H_g$  since this is the ground state hole.

### B. Pulses short compared with nuclear dynamics

We shall now consider the limiting case when the durations of both pulses are short compared to the time scales of the nuclear dynamics of the system. We thus make approximation (i) [Eq. (3.1)] but not (ii). The doorway function  $\hat{D}_m$  [Eq. (2.10)] is simply the spectral convolution of bare doorway  $\hat{D}_m^0$  [Eq. (3.4)] with the spectral profile of

pump field  $|\hat{E}_1|^2$ . Similarly, the window function  $\hat{W}_m$  [Eq. (2.11)] is simply the spectral convolution of bare window  $\hat{W}_m^0$  [Eq. (3.5)] with the spectral profile of pump field  $|\hat{E}_2|^2$ . The signal [Eq. (2.9)] is then given by<sup>40</sup>

$$S(\Omega_1, \Omega_2; \tau) = \int_{-\infty}^{\infty} d\omega_2 \int_{-\infty}^{\infty} d\omega_1 |\hat{E}_2(\omega_2)|^2 |\hat{E}_1(\omega_1)|^2$$

$$\times S_0(\omega_1, \omega_2; \tau). \quad (3.13)$$

### C. Pulses long compared with the electronic dephasing time scale

When the pulses are long compared with the dephasing timescale we make only approximation (ii) [Eq. (3.2)] but not (i). In this case the final signal may be expressed as the temporal convolution of the total intensity of the external fields with the bare spectrum,<sup>40</sup>

$$S(\Omega_1, \Omega_2; \tau) = \int_{-\infty}^{\infty} dt I(\tau - t) S_0(\Omega_1, \Omega_2; t), \quad (3.14a)$$

with

$$I(\tau - t) = \int_{-\infty}^{\infty} dt' |E_2(t')|^2 |E_1(t' + \tau - t)|^2. \quad (3.14b)$$

#### D. Impulsive pump

This is the extreme of the case in Sec. III B, in which we assume that the duration of pump pulse is short compared with both the electronic dephasing and the nuclear dynamics. The pump pulse can either be tuned near resonance or off resonance with respect to the electronic transition. The signal [Eq. (3.13) or (2.9)] in the impulsive pump limit can be expressed as

$$S(\Omega_2; \tau) = \int_{-\infty}^{\infty} d\omega_2 |\hat{E}_2(\omega_2)|^2 \times \{ \text{Tr}[\hat{W}_e^0(\omega_2) \mathcal{G}_{ee}(\tau) \hat{D}_e] \times \text{Tr}[\hat{W}_g^0(\omega_2) \mathcal{G}_{gg}(\tau) \hat{D}_g] \}. \quad (3.15)$$

Here we have assumed that the probe pulse is short compared to the nuclear dynamics of the system (Sec. III B).  $\hat{W}_m^0(\omega_2)$  with  $m = g, e$  is the bare window function [Eq. (3.5)] at frequency  $\omega_2$ . The formal expression of doorway  $\hat{D}_m$  in impulsive pump excitation is different for resonant and off-resonant conditions. In the following, we shall consider the doorway state in both cases.

We shall first consider the doorway state in the *resonant* impulsive pump limit. The analysis of the quantum beat signals in this limit was discussed recently.<sup>16,37</sup> In this case we may represent the pump pulse by a  $\delta$  function

$$E_1(t) = \theta_1 \delta(t) \quad (3.16a)$$

or

$$|\hat{E}_1(\omega_1)|^2 = (2\pi)^{-1} |\theta_1|^2, \quad (3.16b)$$

where  $|\theta_1|$  is the pump pulse area. The doorway for the excited state [Eq. (2.10a)] and for the ground state [Eq. (2.10b)], in the ideal impulsive pump limit, are simply (for  $|\theta_1|^2 = 1$ )

$$\hat{D}_e = 2\mu\rho_g\mu; \quad (3.17a)$$

$$\hat{D}_g = [\mu^2\rho_g + \rho_g\mu^2], \quad |\Omega_1 - \omega_{eg}| \approx \omega_{v'}. \quad (3.17b)$$

We now turn to consider the doorway state in the off-resonant impulsive pump limit.<sup>23</sup> In this limit, the pump pulse is long compared with its inverse detuning; hence it may not be considered to be a  $\delta$  function in time. In this limit, as shown in Eqs. (3.9) and the discussion which followed, the excited-state doorway vanishes and the ground-state doorway retains only its imaginary contribution. Up to a normalization factor, we have

$$\hat{D}_e = 0; \quad (3.18a)$$

$$\hat{D}_g = i[\mu^2\rho_g - \rho_g\mu^2], \quad |\Omega_1 - \omega_{eg}| \gg \omega_{v'}. \quad (3.18b)$$

The off-resonant doorway [Eqs. (3.18)] is purely imaginary whereas the resonant doorway [Eqs. (3.17)] is purely real. In the impulsive limit, the doorway states and the signal do not depend on  $\Omega_1$ . We have therefore omitted the  $\Omega_1$  label in Eqs. (3.15), (3.17), and (3.18). Detailed analysis of the impulsive excitation limit will be presented further in Sec. VI.

#### IV. BROWNIAN OSCILLATOR MODEL FOR NUCLEAR DYNAMICS

In Sec. III we considered several limiting cases in which the probe absorption signal [Eq. (2.9)] may be expressed in terms of the bare spectrum  $S_0$  [Eq. (3.3)], which in turn was expanded in the molecular vibronic eigenstates. Formally this is the simplest representation and it is particularly convenient when only a few vibronic eigenstates have a dominant contribution. When using ultrashort pulses, or when the spectrum of molecular eigenstates is very dense, the eigenstate representation becomes impractical since we need to consider a large number of states. It may then be advantageous to use the Wigner phase space representation, which is particularly suitable for semiclassical approximations.<sup>29,30,45,46</sup> The Wigner representation of an operator  $\hat{A}$  is obtained by the Fourier transformation of the coordinate representation

$$A(\mathbf{p}, \mathbf{q}) \equiv \int_{-\infty}^{\infty} d\mathbf{s} \exp(-i\mathbf{p}\cdot\mathbf{s}) \langle \mathbf{q} + \mathbf{s}/2 | \hat{A} | \mathbf{q} - \mathbf{s}/2 \rangle. \quad (4.1)$$

In Eq. (4.1) and hereafter, we set the Planck constant  $\hbar = 1$ . Using the Wigner representation, the bare spectrum [Eq. (3.3)] can be recast in the form

$$S_0(\Omega_1, \Omega_2; \tau) = \int \int d\mathbf{p} d\mathbf{q} W_e(\Omega_2; \mathbf{p}, \mathbf{q}) D_e(\Omega_1, \tau; \mathbf{p}, \mathbf{q}) + \int \int d\mathbf{p} d\mathbf{q} W_g(\Omega_2; \mathbf{p}, \mathbf{q}) D_g(\Omega_1, \tau; \mathbf{p}, \mathbf{q}). \quad (4.2)$$

The function  $D_m(\Omega_1, \tau; \mathbf{p}, \mathbf{q})$  is the Wigner representations of the bare doorway operator propagated for the time  $\tau$ , i.e.,  $\mathcal{G}_{mm}(\tau) \hat{D}_m^0(\Omega_1)$ , and  $W_m(\Omega_2; \mathbf{p}, \mathbf{q})$  is the Wigner representation of the bare window operator  $\hat{W}_m^0(\Omega_2)$ . We have developed semiclassical equations of motion which allow the numerical computation of these functions for a general system with an arbitrary potential function.<sup>29,30</sup> These equations will be used in the following derivations.

We consider the following model for the molecular Hamiltonian

$$H_g = \frac{1}{2} \sum_j \hbar \omega_j (p_j^2 + q_j^2), \quad (4.3)$$

$$H_e = \frac{1}{2} \sum_j \hbar \omega_j [p_j^2 + (q_j + d_j)^2] + \hbar \omega_{eg}.$$

Here  $p_j$  and  $q_j$  are the dimensionless momentum and coordinate of the  $j$ th nuclear mode with frequency  $\omega_j$ .  $d_j$  is the dimensionless displacement of the equilibrium configurations of this mode in the two electronic potential surfaces.  $q_j$  may represent an intramolecular vibration, an intermolecular libration, a local or a collective solvent motion. We further assume that each mode experiences a Brownian motion with a time-dependent Langevin friction function  $\hat{\gamma}_j(t)$ . The propagation of the doorway function by the  $\mathcal{G}_{mm}(\tau)$  has a well-defined classical analog and can be calculated using the generalized Langevin equations,<sup>30,47-49</sup>

$$\begin{aligned} \dot{q}_j &= \omega_j p_j, \\ \dot{p}_j &= -\omega_j(q_j + \xi d_j) - \int_0^t dt' \hat{\gamma}_j(t-t') p_j(t') + f_j(t). \end{aligned} \quad (4.4)$$

Here  $\hat{\gamma}_j(t)$  is the non-Markovian friction kernel and  $f_j(t)$  represents the Gaussian stochastic random force due to solvent motion acting the  $j$ th mode. They satisfy the fluctuation-dissipation relation:  $\hat{\gamma}_j(t) = k_B T \langle f_j(t) f_j(0) \rangle$ . The parameter  $\xi=0$  for the ground-state ( $m=g$ ) evolution and  $\xi=1$  for the excited-state ( $m=e$ ) evolution. In order to evaluate the doorway [Eq. (3.4)] and the window [Eq. (3.5)] functions, we need to propagate the system also for the  $t_1$  and  $t_3$  periods, in which the system is in an electronic coherence. The generalization of the Langevin equations [Eq. (4.4)] to the  $t_1$  and  $t_3$  periods was made recently.<sup>30</sup> For simplicity we shall further invoke the Condon approximation, in which the electronic transition dipole depends weakly on the nuclear coordinate, and we set  $\mu(q_j) = \mu_j$  independent of  $q_j$ . Making use of our semiclassical equations of motion,<sup>30</sup> we obtained the following exact expressions for the doorway and the window functions for our harmonic model system:

$$D_g(\Omega_1, \tau; p, q) = 2 \operatorname{Re} \int_0^\infty dt_1 \exp[i(\Omega_1 - \omega_{eg})t_1] \times \prod_j F_{gj}(t_1, \tau; p_j, q_j), \quad (4.5a)$$

$$W_g(\Omega_2; p, q) = 2 \operatorname{Re} \int_0^\infty dt_3 \exp[i(\Omega_2 - \omega_{eg})t_3] \times \prod_j G_{gj}(t_3; p_j, q_j). \quad (4.5b)$$

$D_e$  and  $W_e$  are given by similar expressions with changing  $F_{gj}$  and  $G_{gj}$  to  $F_{ej}$  and  $G_{ej}$ . The doorway function  $F_{gj}(t_1, \tau; p_j, q_j)$  can be obtained as follows. The system starts with the equilibrium ground-state density-matrix distribution  $F_{gj}(0, \tau, p_j, q_j) = \rho_g(p_j, q_j)$ . It then propagates for the time period  $t_1$  when the system is in the electronic coherence

$$F_{gj}(t_1, 0; p_j, q_j) = \exp(-iH_e t_1) F_{gj}(0, 0; p_j, q_j) \exp(iH_g t_1).$$

Finally, the system propagates for the time period  $\tau$  in the electronic ground ( $m=g$ ) state, resulting in

$$F_{gj}(t_1, \tau; p_j, q_j) = \exp(-iH_g \tau) F_{gj}(t_1, 0; p_j, q_j) \exp(iH_g \tau).$$

The function  $F_{ej}$  can be obtained in a similar way except that the final propagation for the  $\tau$  period in the electronic excited ( $m=e$ ) state. The window function is calculated by starting with the phase-space distribution  $\delta(p'_j - p_j) \delta(q'_j - q_j)$ , which then propagates for the time period  $t_3$  in the electronic coherence

$$\exp(-iH_e t_3) \delta(p'_j - p_j) \delta(q'_j - q_j) \exp(iH_g t_3).$$

$G_{gj}(t_3; p_j, q_j)$  is then obtained by integrating the resulting distribution over  $p'_j, q'_j$ . Note that within the Condon approximation the ground-state and the excited-state window functions are identical, i.e.,  $G_{gj} = G_{ej}$ . Using Eq. (3.12) of Ref. 30, we obtain, for the ground doorway and window functions in the harmonic Brownian oscillator model,

$$F_{gj}(t_1, \tau; p_j, q_j) = \frac{|\mu_j|^2}{\pi(2\bar{n}_j + 1)} \exp[-g_j(t_1)] \times \exp\left[-\frac{(q_j - \bar{q}_j)^2 + (p_j - \bar{p}_j)^2}{2\bar{n}_j + 1}\right], \quad (4.6a)$$

$$G_{gj}(t_3; p_j, q_j) = |\mu_j|^2 \exp[-g_j(t_3)] \times \exp(\eta_0 + i\eta_1 q_j + i\eta_2 p_j), \quad (4.6b)$$

with

$$\bar{n}_j = [\exp(\hbar\omega_j/k_B T) - 1]^{-1}, \quad (4.7a)$$

$$g_j(t) = \frac{i}{2} d_j^2 \omega_j \int_0^t dt' M_j(t') + (\bar{n}_j + \frac{1}{2}) d_j^2 \omega_j^2 \int_0^t dt' \int_0^{t'} dt'' M_j(t''), \quad (4.7b)$$

$$\begin{aligned} \begin{bmatrix} \bar{q}_j \\ \bar{p}_j \end{bmatrix} &= \frac{1}{2} d_j \mathcal{I}(\tau) \begin{bmatrix} M_j(t_1) - 1 \\ \omega_j^{-1} \dot{M}_j(t_1) \end{bmatrix} \\ &- i(\bar{n}_j + \frac{1}{2}) d_j \mathcal{I}(\tau) \begin{bmatrix} \omega_j \int_0^{t_1} dt' M_j(t') \\ M_j(t_1) - 1 \end{bmatrix} \\ &+ \xi d_j \begin{bmatrix} M_j(\tau) - 1 \\ \omega_j^{-1} \dot{M}_j(\tau) \end{bmatrix}, \end{aligned} \quad (4.7c)$$

and

$$\eta_0 = (\bar{n}_j + \frac{1}{2}) d_j^2 \omega_j^2 \times \int_0^{t_3} dt' \int_0^{t'} dt'' [\mathcal{I}(t' - t'') \mathcal{I}(t'') \mathcal{I}^\dagger(t'') ]_{11}, \quad (4.8a)$$

$$\eta_1 = -d_j \omega_j \int_0^{t_3} dt' M_j(t'), \quad (4.8b)$$

$$\eta_2 = d_j [M_j(t_3) - 1], \quad (4.8c)$$

where

$$\mathcal{I}(t) \equiv \begin{bmatrix} M_j(t) & -\omega_j^{-1} \dot{M}_j(t) \\ \omega_j^{-1} \dot{M}_j(t) & -\omega_j^{-2} \ddot{M}_j(t) \end{bmatrix}, \quad (4.9a)$$

$$\begin{aligned} M_j(t) &= \frac{\frac{1}{2} \langle q_j(t) q_j + q_j q_j(t) \rangle - \langle q_j \rangle^2}{\langle q_j^2 \rangle - \langle q_j \rangle^2} \\ &= L^{-1} \left[ \frac{s + \gamma_j(s)}{s^2 + s\gamma_j(s) + \omega_j^2} \right]. \end{aligned} \quad (4.9b)$$

The parameter  $\xi$  in Eq. (4.7c) is  $\xi=0$ . The excited-state functions  $F_{ej}$  and  $G_{ej}$  are given by the same expressions by setting  $\xi=1$ .  $\bar{n}_j$  [Eq. (4.7a)] denotes the thermal occupation number of the  $j$ th mode with  $k_B$  being the Boltzmann constant and  $T$  being the temperature. In Eq. (4.9b) both the time evolution and the thermal average  $\langle \rangle$  are with respect to the ground-state Hamiltonian.  $L^{-1}$  denotes the inverse Laplace transform with  $s$  being the Laplace variable conjugate to time  $t$ , and  $\gamma_j(s)$  is the Langevin friction in the Laplace space. In Eq. (4.8a), the dagger superscript denotes the Hermitian conjugate, and  $[ ]_{11}$  denotes the (1,1) matrix element. In the present

model, the time evolution of the  $j$ th mode depends entirely on its correlation function  $M_j(t)$  [Eq. (4.9b)], which in turn depends on its harmonic frequency  $\omega_j$  and the friction function  $\gamma_j(s)$ . It can easily be shown that  $M_j(t)$  satisfies the equation of motion,

$$\ddot{M}_j(t) + \int_0^t dt' \hat{\gamma}_j(t-t') \dot{M}_j(t') + \omega_j^2 M_j(t) = 0. \quad (4.10)$$

The frequency dependence of  $\gamma_j(s)$  reflects the time

scales of the thermal motions of the bath responsible for the random force. If these motions are very fast compared with the oscillator motion, the  $s$  dependence of  $\gamma_j(s)$  is very weak and can be neglected, i.e.,

$$\gamma_j(s) = \gamma_j(s=0) \equiv \gamma_j. \quad (4.11)$$

In this case we can perform the inverse Laplace transform in Eq. (4.9b) resulting in

$$M_j(t) = \begin{cases} \exp(-\gamma_j t/2) \left[ \cos \bar{\omega}_j t + \frac{\gamma_j}{2\bar{\omega}_j} \sin \bar{\omega}_j t \right], & \gamma_j < 2\omega_j \\ \exp(-\gamma_j t/2) (1 + \gamma_j t/2), & \gamma_j = 2\omega_j \\ \frac{s_+}{s_+ - s_-} \exp(-s_- t) - \frac{s_-}{s_+ - s_-} \exp(-s_+ t), & \gamma_j > 2\omega_j \\ \exp(-\Lambda_j t), & \gamma_j \gg 2\omega_j. \end{cases} \quad (4.12a)$$

Here

$$\bar{\omega}_j = [\omega_j^2 - (\gamma_j/2)^2]^{1/2}, \quad (4.13a)$$

$$s_{\pm} = \gamma_j/2 \pm [(\gamma_j/2)^2 - \omega_j^2]^{1/2}, \quad (4.13b)$$

$$\Lambda_j = \omega_j^2 / \gamma_j. \quad (4.13c)$$

Equations (4.12a)–(4.12d) represent an underdamped, critically damped, overdamped, and strongly overdamped oscillator, respectively. Equations (4.6)–(4.13) will be used in the following sections.

#### V. STRONGLY OVERDAMPED NUCLEAR MOTIONS: LOW-FREQUENCY MODES AND SOLVATION DYNAMICS

In the last section we presented the doorway and the window functions for the multimode Brownian oscillator system. Equations (4.5)–(4.9) are the key ingredients for calculating the probe absorption spectrum of polyatomic molecules (whether isolated or in condensed phases). Low-frequency molecular modes and solvent modes are usually strongly overdamped (i.e., the friction is much larger than the relevant frequency). Consequently, they do not show up in the spectra as progressions of well resolved lines but rather contribute to line broadening. Spectra of polyatomic molecules in condensed phases are dominated by the broadening modes.<sup>28</sup> In this section we shall analyze in detail the low-frequency contributions for which the expressions for the doorway and the window functions are greatly simplified. Consider a low-frequency mode  $q_j$ . It couples to the optical transition through this contribution to the difference between  $H_e$  and  $H_g$ . (If the difference vanishes, that mode does not couple to the electronic transition and is irrelevant). We thus introduce the coordinate

$$U_j \equiv H_e(p_j, q_j) - H_g(p_j, q_j) - \hbar \omega_{eg}. \quad (5.1a)$$

Using the Hamiltonian [Eq. (4.3)] we then have

$$U_j = d_j \omega_j (q_j + d_j/2). \quad (5.1b)$$

We assume that the Langevin friction acting on  $U_j$  is much larger than its frequency  $\gamma_j(s) \gg \omega_j$ . Consequently,  $\gamma_j(s)$  is also much larger than the relevant frequency for  $M_j(t)$ , i.e.,  $\gamma_j(s) \gg s$ . Equation (4.9b) thus becomes, in this case,

$$M_j(t) = \frac{\frac{1}{2} \langle U_j(t) U_j + U_j U_j(t) \rangle - \langle U_j \rangle^2}{\langle U_j^2 \rangle - \langle U_j \rangle^2} = L^{-1} \left[ \frac{1}{s + \Lambda_j(s)} \right], \quad (5.2)$$

with  $\Lambda_j(s) \equiv \omega_j^2 / \gamma_j(s)$ . Equation (5.2) can also be obtained from Eq. (4.10) by neglecting  $\ddot{M}_j(t)$ . Since in this case the momentum rapidly attains its equilibrium value and need not be considered an independent dynamical variable, the oscillator distribution function satisfied a Smoluchowski equation in configuration space<sup>30,48–50</sup> (rather than a Fokker-Planck equation in phase space). The phase-space doorway and the window functions in Eqs. (4.5) reduce to functions  $F_{mj}(t_1, \tau; U_j)$  and  $G_{mj}(t_3; U_j)$  in the coordinate space. Furthermore, the phase-space integration over  $p_j q_j$  in Eq. (4.2) is replaced by an integration over the coordinate  $U_j$ . Hereafter, we refer to  $U_j$  as the strongly overdamped mode (SOM). We thus get

$$F_{gj}(t_1, \tau; U_j) = (2\pi \Delta_j^2)^{-1/2} \times \exp[-\frac{1}{2}(U_j - \bar{U}_j)^2 / \Delta_j^2 - g_j(t_1)], \quad (5.3a)$$

$$G_{gj}(t_3; U_j) = \exp(-i U_j c_j - b_j). \quad (5.3b)$$

Here

$$\lambda_j = \langle U_j \rangle = \frac{1}{2} d_j^2 \omega_j, \quad (5.4a)$$

$$\Delta_j^2 = \langle U_j^2 \rangle - \langle U_j \rangle^2 = (\bar{n}_j + \frac{1}{2}) d_j^2 \omega_j^2 \approx 2k_B T \lambda_j. \quad (5.4b)$$

The last (approximate) equality in Eq. (5.4b) is derived using the fluctuation-dissipation theorem, in the high-temperature limit (i.e., when  $k_B T$  is much larger than the relevant frequency scale of the  $U_j$  coordinate). The function  $g_j(t)$  [Eq. (4.7b)] is the line broadening function induced by this strongly overdamped coordinate,<sup>28,30</sup>

$$g_j(t_1) = i\lambda_j \int_0^{t_1} dt' M_j(t') + \Delta_j^2 \int_0^{t_1} dt' \int_0^{t'} dt'' M_j(t''). \quad (5.5a)$$

We further have

$$\bar{U}_j = (1 - 2\xi)\lambda_j [1 - M_j(\tau)] + \lambda_j M_j(\tau) M_j(t_1) - i\Delta_j^2 M_j(\tau) \int_0^{t_1} dt' M_j(t'), \quad (5.5b)$$

$$b_j = \Delta_j^2 \int_0^{t_3} dt' \int_0^{t'} dt'' M_j(t' - t'') [1 - M_j^2(t'')], \quad (5.5c)$$

$$c_j = \int_0^{t_3} dt' M_j(t'). \quad (5.5d)$$

The parameter  $\xi$  was introduced in Eq. (4.4). For  $F_{gj}$  and  $G_{gj}$  we set  $\xi=0$ . The excited-state functions  $F_{ej}$  and  $G_{ej}$  are given by the same equations with  $\xi=1$ . The parameter  $\bar{U}_j$  depends on  $\tau$  and  $t_1$ , whereas the parameters  $c_j$  and  $b_j$  depend on  $t_3$ . Equations (5.2)–(5.5) show that the effect of an overdamped mode on the spectrum depends on a single static quantity  $\lambda_j$  [Eq. (5.4a)] and the dynamical (normalized and real) correlation function  $M_j(t)$  [Eq. (5.2)].<sup>32–36,44</sup> This is to be contrasted with a general underdamped vibration which requires two static parameters ( $d_j$  and  $\omega_j$ ) in addition to  $M_j(t)$ . The significance of  $\lambda_j$  may be demonstrated by considering the linear absorption and the fluorescence line shapes, in the present model, which are given by<sup>28</sup>

$$\sigma_A(\omega) = \frac{1}{\pi} \text{Re} \int_0^\infty dt \exp[i(\omega - \omega_{eg})t] \exp[-g(t)], \quad (5.6a)$$

$$\sigma_F(\omega) = \frac{1}{\pi} \text{Re} \int_0^\infty dt \exp[i(\omega - \omega_{eg})t] \exp[-g^*(t)]. \quad (5.6b)$$

Note that  $\sigma_F(-\omega) = \sigma_A(\omega)$  so that  $\sigma_F$  is the mirror image of  $\sigma_A$ .  $\lambda_j$  is related to a spectral shift between the absorption and the emission. In the spectral diffusion limit considered below we shall show that the red shift of the fluorescence with respect to the absorption (i.e., the Stokes shift<sup>36,44,51</sup>) is equal to  $2\lambda_j$ . In the present model,  $U_j$  may represent not only a single molecular vibration but also a collective *solvation coordinate*<sup>36,44</sup> defined as the difference between  $H_e$  and  $H_g$  resulting from a group of solvent degrees of freedom. Since the solvation coordinate is a sum of a large number of small contributions from individual solvent molecules, we may invoke the central limit theorem and assume that it satisfies Gaussian statistics and the Smoluchowski equation. As an example we may consider a polar solute in a polar medium. In that case we have<sup>36,50</sup>

$$U_j = - \int d\mathbf{r} \Phi_{eg}(\mathbf{r}) P(\mathbf{r}), \quad (5.7)$$

where  $P(\mathbf{r})$  is the solvent polarization and  $\Phi_{eg}(\mathbf{r})$  is the difference in the electric fields at point  $\mathbf{r}$  created by the chromophore charge distribution when it is in the electronic excited state  $|e\rangle$  and in the ground state  $|g\rangle$ . In the dielectric continuum model,<sup>50</sup> we get: [cf. Eq. (5.4a) and (5.2)]

$$\lambda_j = \frac{1}{8\pi} \int d\mathbf{r} |\Phi_{eg}(\mathbf{r})|^2 \left[ \frac{1}{\epsilon_\infty} - \frac{1}{\epsilon_0} \right], \quad (5.8a)$$

$$M_j(t) = \frac{1}{2\pi i} \int_{-\infty}^\infty \frac{d\omega}{\omega} \exp(i\omega t) \frac{1/\epsilon(\omega) - 1/\epsilon_0}{1/\epsilon_\infty - 1/\epsilon_0}. \quad (5.8b)$$

Here  $\epsilon_0$  is the static ( $\omega=0$ ), and  $\epsilon_\infty$  is the high-frequency (optical) value of  $\epsilon(\omega)$ . Solvation structure may be included using the wave vector and frequency-dependent dielectric function  $\epsilon(\mathbf{k}, \omega)$ .<sup>50,52,53</sup>

We shall consider now some limiting cases and present explicit expressions for the SOM contribution to the doorway and to the window functions.

#### A. Spectral diffusion: From hole burning to the impulsive limit

When the line shapes are broad (fast dephasing) and the SOM motion is much slower than the dephasing time scale, we can neglect the SOM nuclear dynamics during the electronic transition in the time intervals  $t_1$  and  $t_3$ .<sup>36,44</sup> We then have  $b_j=0$  and  $c_j=t_3$  in Eq. (5.5), and Eq. (5.3) with

$$g_j(t_1) = i\lambda_j t_1 + \frac{1}{2} \Delta_j^2 t_1^2, \quad (5.9a)$$

$$\bar{U}_j = (1 - 2\xi)\lambda_j [1 - M_j(\tau)] + \lambda_j M_j(\tau) - i\Delta_j^2 M_j(\tau) t_1, \quad (5.9b)$$

$$G_{gj}(t_3; U_j) = \exp(-iU_j t_3). \quad (5.9c)$$

The absorption [Eq. (5.6a)] and the fluorescence [Eq. (5.6b)] line shapes are inhomogeneously broadened in this case, i.e.,

$$\sigma_A(\omega) = (2\pi\Delta_j^2)^{-1/2} \exp[-(\omega - \omega_{eg} - \lambda_j)^2 / 2\Delta_j^2], \quad (5.10a)$$

$$\sigma_F(\omega) = (2\pi\Delta_j^2)^{-1/2} \exp[-(\omega - \omega_{eg} + \lambda_j)^2 / 2\Delta_j^2]. \quad (5.10b)$$

The Stokes shift, which is the difference between the absorption and the fluorescence peaks, is equal to  $2\lambda_j$ . The SOM dynamics can be clearly seen if we substitute Eqs. (5.9), (5.3a), and (4.5) into (4.2) and (3.13) (ignoring for a moment the contribution of the other modes). In this case we recover the classical limit [Eq. (3.12)] with Gaussian statistics.<sup>50</sup> If we further take the pump and probe spectral profiles  $|\hat{E}_1(\omega_1)|^2$  and  $|\hat{E}_2(\omega_2)|^2$  to be Gaussian with variances  $w_1$  and  $w_2$ , respectively, we obtain

$$\begin{aligned}
S(\Omega_1, \Omega_2; \tau) &= 2\pi[(\Delta_j^2 + w_1^2)\alpha^2(\tau)]^{-1/2} \\
&\times \exp[-(\Omega_1 - \omega_{eg} - \lambda_j)^2 / 2(\Delta_j^2 + w_1^2)] \\
&\times (\exp\{-[\Omega_2 - \Omega_e(\tau)]^2 / 2\alpha^2(\tau)\} \\
&+ \exp\{-[\Omega_2 - \Omega_g(\tau)]^2 / 2\alpha^2(\tau)\}), \quad (5.11a)
\end{aligned}$$

$$\Omega_e(\tau) \equiv \omega_{eg} - \lambda_j + M_j(\tau)(\Omega_0 - \omega_{eg} + \lambda_j), \quad (5.11b)$$

$$\Omega_g(\tau) \equiv \omega_{eg} + \lambda_j + M_j(\tau)(\Omega_0 - \omega_{eg} - \lambda_j), \quad (5.11c)$$

$$\Omega_0 \equiv \Omega_1 \frac{\Delta_j^2}{\Delta_j^2 + w_1^2} + (\omega_{eg} + \lambda_j) \frac{w_1^2}{\Delta_j^2 + w_1^2}, \quad (5.11d)$$

$$\alpha^2(\tau) \equiv \Delta_j^2 \left[ 1 - \frac{\Delta_j^2}{\Delta_j^2 + w_1^2} M_j^2(\tau) \right] + w_2^2. \quad (5.11e)$$

The probe absorption has two contributions. The first term in the bold parentheses in Eq. (5.11a) represents the excited “particle” dynamic whereas the second term represents the ground-state “hole” dynamics. At zero delay  $\tau=0$  both terms are identical. They are Gaussians centered at  $\Omega_2 = \Omega_0$  and with a variance  $\alpha(0)$ . As the delay time is increased, the particle and the hole undergo diffusive dynamics on the appropriate potential surfaces (the excited state for the particle and the ground state for the hole). The probe absorption then splits into two contributions centered at  $\Omega_e(\tau)$  for the particle and  $\Omega_g(\tau)$  for the hole. This splitting represents the time development of the Stokes shift. At long times we have  $\Omega_e(\infty) = \omega_{eg} - \lambda_j$  and  $\Omega_g(\infty) = \omega_{eg} + \lambda_j$ . These terms then reflect the stationary fluorescence and absorption [Eq. (5.10)] and their splitting is the Stokes shift  $2\lambda_j$ . The magnitude and sign of the particle and the hole spectral shifts depend on the pump frequency  $\Omega_1$ . For resonance pump excitation  $\Omega_1 = \omega_{eg} + \lambda_j$  (or  $\Omega_0 = \omega_{eg} + \lambda_j$ ), the particle experiences a time-dependent red shift from  $\Omega_2 = \omega_{eg} + \lambda_j$  to  $\Omega_2 = \omega_{eg} - \lambda_j$ . The hole position, in this case, does not evolve in time. When  $\Omega_1 = \omega_{eg} - \lambda_j(1 + 2w_1^2/\Delta_j^2)$  (or  $\Omega_0 = \omega_{eg} - \lambda_j$ ), the particle does not shift in time while the hole undergoes a blue shift from  $\Omega_2 = \omega_{eg} - \lambda_j$  to  $\Omega_2 = \omega_{eg} + \lambda_j$ . In general, both particle and hole contributions undergo time-dependent shifts, as illustrated in Fig. 3.  $\alpha(\tau)$  represents the time-dependent spectral width of the particle and the hole. This width increases with time with the values

$$\alpha(0) = [\Delta_j^2 w_1^2 / (\Delta_j^2 + w_1^2) + w_2^2]^{1/2}, \quad (5.12a)$$

$$\alpha(\infty) = (\Delta_j^2 + w_2^2)^{1/2}. \quad (5.12b)$$

In the impulsive pump limit (Sec. III D) where  $w_1 \gg \Delta_j$ , we have  $\Omega_0 = \omega_{eg} + \lambda_j$  and  $\alpha(0) \approx (\Delta_j^2 + w_2^2)^{1/2} = \alpha(\infty)$ . In this case only the particle experiences a red shift. The spectral width, as well as the hole position, do not evolve in time. In the other extreme limit where  $w_1$  and  $w_2 \ll \Delta_j$ , we have  $\alpha(0) \approx (w_1^2 + w_2^2)^{1/2} \ll \alpha(\infty)$ . The spectral width, in this case, shows a diffusive broadening. In this limit the pump-probe technique is usually referred

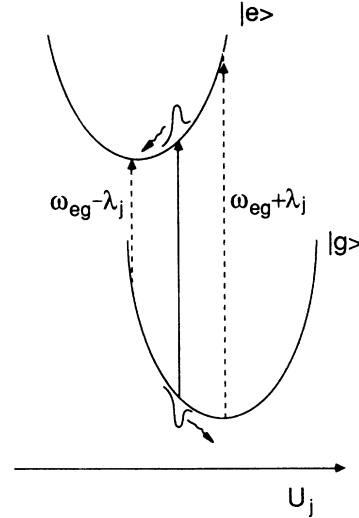


FIG. 3. The dynamical Stokes shift for a strongly overdamped mode  $U_j$  in the spectral diffusion limit [Eq. (5.11)]. The potential function for the  $U_j$  mode has a displaced equilibrium position in the ground and in the excited electronic states. For  $\Omega_0 > \omega_{eg} - \lambda_j$  ( $\Omega_0 < \omega_{eg} - \lambda_j$ ) the particle relaxation in the electronic excited state results in a red (blue) shift of the probe absorption. For  $\Omega_0 > \omega_{eg} + \lambda_j$  ( $\Omega_0 < \omega_{eg} + \lambda_j$ ) the hole relaxation in the electronic ground state shows a red (blue) shift. The solid line represents a pump excitation in which  $\omega_{eg} - \lambda_j < \Omega_0 < \omega_{eg} + \lambda_j$ . In this case, the excited “particle” relaxation shows a red shift while the ground state “hole” shows a blue shift.

to as “hole burning.” The name implies that the pump pulse burns a narrow hole in the SOM distribution since it interacts only with a small subgroup of the ensemble. As time evolves the hole fills, eventually acquiring the equilibrium value  $\alpha(\infty) \approx \Delta_j$ . Finally, we note that the signal is sensitive to the spectral linewidth  $w_2$  of the probe pulse. That width determines the spectral width of the window. For impulsive probe,  $w_2 \rightarrow \infty$  and  $\alpha(\tau) \rightarrow \infty$  and the signal loses its time dependence, i.e., the probe absorption does not depend on  $\tau$ . The probe pulse must be, therefore, sufficiently long to allow for spectral selectivity in the detection process. For that reason, experiments using impulsive probes usually adopt the dispersed detection mode  $S'$  [Eq. (2.4b)] instead of the integrated signal  $S$  [Eq. (2.4a)].

## B. The Markovian limit

In many cases, the Langevin random force in Eq. (4.4) has a very short correlation time compared with the oscillator dynamics. In this limit we can neglect the frequency dependence of the friction  $\gamma_j(s)$  and assume  $\Lambda_j(s) \equiv \Lambda_j$  is independent of  $s$ . The SOM correlation function [Eq. (5.2)] then reduces to

$$M_j(t) = \exp(-\Lambda_j t). \quad (5.13)$$

Equation (5.13) may also be obtained by considering a polar solvent with a Debye dielectric function. Equation (5.8b) then yields Eq. (5.13) with  $\Lambda_j^{-1}$  being the Debye

longitudinal relaxation time.<sup>54</sup> This limit also represents the well-known stochastic model of spectral line broadening,<sup>55</sup> where the oscillator motion is described by the Smoluchowski equation. Our expression includes, however, a time-dependent spectral shift, the Stokes shift, given by the imaginary part of  $g_j(t_1)$  [Eq. (5.5a)], which is absent in the stochastic model. This model has the following additional limits.<sup>28</sup>

### 1. Static (inhomogeneous) broadening

When  $\Delta_j \gg \Lambda_j$  the molecular dynamics is very slow and can be neglected on the relevant time scale. We thus set  $M_j(t) = 1$ . The probe absorption is then given by an average over the inhomogeneous distribution with Eq. (5.10a) for the 0-0 electronic transition frequency.

### 2. Homogeneous broadening

In the opposite extreme  $\Lambda_j \gg \Delta_j$ , the molecular motions are very fast. We can then set

$$M_j(t) = (2/\Lambda_j)\delta(t), \quad (5.14a)$$

and we have [cf. Eq. (5.5)]

$$g_j(t) = i(\lambda_j/\Lambda_j) + \hat{\Gamma}_j t, \quad (5.14b)$$

with

$$\hat{\Gamma}_j \equiv \Delta_j^2/\Lambda_j. \quad (5.14c)$$

The absorption line shape [Eq. (5.6a)] is given by

$$\sigma_A(\omega) = \frac{1}{\pi} \frac{\hat{\Gamma}_j \cos(\lambda_j/\Lambda_j) + (\omega - \omega_{eg}) \sin(\lambda_j/\Lambda_j)}{(\omega - \omega_{eg})^2 + \hat{\Gamma}_j^2}. \quad (5.15)$$

The fluorescence line shape [Eq. (5.6b)] is given by the same expression, with the replacement of  $\lambda_j$  by  $-\lambda_j$ . When  $\lambda_j \ll \Lambda_j$ , these line shapes assume the Lorentzian form with the width equal to the dephasing rate  $\hat{\Gamma}_j$ . The Stokes shift vanishes in this case due to the rapid motion of the SOM. The contributions of the solvation coordinate to the doorway and window functions are in this case

$$F_{gj}(t_1, \tau; U_j) = \exp(-\hat{\Gamma}_j t_1) (2\pi\Delta_j^2)^{-1/2} \times \exp[-\frac{1}{2}(U_j - \lambda_j)^2/\Delta_j^2], \quad (5.16a)$$

$$G_{gj}(t_3; U_j) = \exp(-\hat{\Gamma}_j t_3). \quad (5.16b)$$

$F_{ej}$  and  $G_{ej}$  are given by the same expressions by replacing  $U_j - \lambda_j$  with  $U_j + \lambda_j$ . It is interesting to note that in the homogeneous limit we do not need to consider the solvation coordinate  $U_j$  explicitly in Eq. (4.2). We can perform the  $U_j$  integration which simply results in the replacement of  $\omega_{eg}$  by  $\omega_{eg} - i\hat{\Gamma}_j$ . We can therefore perform the  $U_j$  integration in Eq. (4.2) while maintaining the simple doorway-window picture. This is generally not the case for modes  $U_j$  which are not in the homogeneous limit.

## VI. IMPULSIVE SPECTROSCOPY AND QUANTUM BEATS

Recently, the impulsive optical excitation technique has been widely used for probing the coherent nuclear dynamics of chromophores in condensed phases.<sup>3-14,16</sup> In this section we analyze the probe absorption signal [Eq. (3.15)] for the Brownian oscillator model introduced in Sec. IV, in the impulsive pump limit. For simplicity we first consider the case in which the probe field is short compared with the molecular nuclear dynamics [Eq. (3.1)], but is long compared with the dephasing time scale [Eq. (3.2b)]. In this case, Eq. (3.15) yields (up to a proportionality constant)

$$S(\Omega_2; \tau) = 2 \operatorname{Re} \int_0^\infty dt_3 \exp(i\Omega_2 t_3) [J_e(t_3; \tau) + J_g(t_3; \tau)], \quad (6.1)$$

with

$$J_e(t_3; \tau) = \operatorname{Tr}[\mu \exp(-iH_e t_3) \hat{D}_e(\tau) \mu \exp(iH_g t_3)], \quad (6.2a)$$

$$J_g(t_3; \tau) = \operatorname{Tr}[\mu \exp(-iH_e t_3) \mu \hat{D}_g(\tau) \exp(iH_g t_3)], \quad (6.2b)$$

and

$$\hat{D}_e(\tau) = \mathcal{G}_{ee}(\tau) \hat{D}_e \equiv \exp(-iH_e \tau) \hat{D}_e \exp(iH_e \tau), \quad (6.3a)$$

$$\hat{D}_g(\tau) = \mathcal{G}_{gg}(\tau) \hat{D}_g \equiv \exp(-iH_g \tau) \hat{D}_g \exp(iH_g \tau). \quad (6.3b)$$

In deriving Eq. (6.1), we made use of Eq. (3.5) for the window state.  $J_e$  and  $J_g$  [Eq. (6.2)] are two time correlation functions of the dipole operator calculated with respect to the nonequilibrium oscillator distribution functions  $\hat{D}_e(\tau)$  and  $\hat{D}_g(\tau)$  [Eq. (6.3)], respectively. In Eqs. (6.3), the doorway state  $\hat{D}_m$  is given by Eqs. (3.17) for the resonant pump configuration, or by Eqs. (3.18) for the off-resonant pump excitation.

We shall consider the effect of Condon approximation on the probe absorption signal. Let us first consider the signal in the resonant impulsive pump limit [Eqs. (6.1)–(6.3) and (3.17)]. In general, the electronic dipole  $\mu$  depends on the nuclear coordinates. Consequently, both the excited doorway  $\hat{D}_e(\tau)$  (particle) and the ground doorway  $\hat{D}_g(\tau)$  (hole) vary with the delay time  $\tau$ . However, in the Condon approximation, in which  $\mu$  is assumed to be independent of the nuclear coordinate, the hole ( $\hat{D}_g$ ) will no longer vary with  $\tau$ . In this case only the excited-state dynamics as given by  $\hat{D}_e(\tau)$ , are probed.<sup>37</sup> We shall consider this case first in Sec. VIA. Later, in Sec. VIB, we shall consider off-resonance pumping [Eqs. (6.1)–(6.3) and (3.18)], in which only the ground-state dynamics are retained and the non-Condon effects are essential.

### A. Impulsive resonant excitation

We first consider the impulsive optical signal [Eq. (6.1)] of the Brownian oscillator model in the Condon approximation, where  $\mu = \mu_{eg}$  is independent of the nuclear coordinates. The key quantities which determine the impulsive optical signal are the two time correlation functions  $J_e$  and  $J_g$  [Eqs. (6.2), (6.3), and (3.17)]. Their calculation

requires propagating the molecular system in the electronic coherence  $|e\rangle\langle g|$  during the  $t_3$  period, as well as in electronic population  $|e\rangle\langle e|$  or  $|g\rangle\langle g|$  during the delay time  $\tau$  period. For the harmonic Brownian oscillator model [Eqs. (4.3) and (4.4)] in the Condon approximation, we have<sup>30,37</sup>

$$J_e(t_3; \tau) = |\mu_{eg}|^4 \exp(-i\omega_{eg}t_3) \times \exp\left[-\sum_j [g_j^*(t_3) + f_j(t_3; \tau)]\right], \quad (6.4a)$$

$$J_g(t_3; \tau) = |\mu_{eg}|^4 \exp(-i\omega_{eg}t_3) \exp\left[-\sum_j g_j(t_3)\right]. \quad (6.4b)$$

Here

$$f_j(\tau; t_3) = i(2\lambda_j/\omega_j^2)\dot{M}_j(\tau)[1 - M_j(t_3)] + i2\lambda_j M_j(\tau) \int_0^{t_3} dt' M_j(t'), \quad (6.5a)$$

$$g_j(t_3) = i\lambda_j \int_0^{t_3} dt' M_j(t') + \Delta_j^2 \int_0^{t_3} dt' \int_0^{t'} dt'' M_j(t''), \quad (6.5b)$$

and

$$\lambda_j = \frac{1}{2}d_j^2\omega_j, \quad (6.6a)$$

$$\Delta_j^2 = (\bar{n}_j + \frac{1}{2})d_j^2\omega_j^2. \quad (6.6b)$$

Equation (6.5b) is identical to Eq. (4.7b). Note that within the Condon approximation  $J_g(\tau_3; \tau)$  [Eq. (6.4b)] does not depend on the time delay  $\tau$ .  $M_j$  is the normalized correlation function of the  $j$ th mode [Eq. (4.9b) or (5.2)]. It should further be noted that  $J_e(t_3; 0) = J_g(t_3; 0)$ ; hence, at short delay times, the two contributions in Eq. (6.1) are identical. In the presence of friction,  $f_j(t_3; \infty) = 0$ ; hence, for long delay times, the signal [Eq. (6.1)] splits into two components with reflection symmetry, i.e., the contribution of  $J_g$  at  $\Omega_2 - \omega_{eg}$  equals the contribution of  $J_e$  at  $-(\Omega_2 - \omega_{eg})$ . The calculation of the impulsive optical signal of polyatomic molecules in condensed phases using Eqs. (6.1) and (6.4) has been reported elsewhere.<sup>37</sup>

One of the most remarkable features of impulsive spectroscopy of solvated dyes is the appearance of simple damped harmonic beats with only a few fundamental vibrational frequencies and with a very small contribution of overtones.<sup>11-13,16,37</sup> Equations (6.4)–(6.6) provide a general framework for analyzing these effects. To that end we shall expand Eq. (6.4a) in the form

$$J_e(t_3; \tau) = J_e(t_3; \infty) \sum_{n=0}^{\infty} \frac{(-1)^n}{n!} \left[ \sum_j f_j(t_3; \tau) \right]^n. \quad (6.7)$$

Truncating this expansion at first order ( $n=1$ ), Eq. (6.1) yields

$$S(\Omega_2; \tau) \approx S(\Omega_2; \infty) + 2|\mu_{eg}|^4 \sum_j [M_j(\tau)A_j(\Omega_2) + \dot{M}_j(\tau)B_j(\Omega_2)]. \quad (6.8a)$$

Here

$$A_j(\Omega_2) = 2\lambda_j \text{Im} \int_0^{\infty} dt_3 \int_0^{t_3} dt' \exp(i\Omega_2 t_3) \times J_e(t_3; \infty) M_j(t'), \quad (6.8b)$$

$$B_j(\Omega_2) = (d_j^2/\omega_j) \text{Im} \int_0^{\infty} dt_3 \exp(i\Omega_2 t_3) J_e(t_3; \infty) \times [1 - M_j(t_3)]. \quad (6.8c)$$

$S(\Omega_2; \infty)$  is given by Eq. (6.1) by sending  $\tau \rightarrow \infty$ . It consists of a contribution from  $J_g$  and from  $J_e(t_3, \infty)$ , which have a reflection symmetry around  $\Omega_2 = \omega_{eg}$ . The second term in Eq. (6.8a) results from the first-order ( $n=1$ ) contribution to Eq. (6.7), and depends on the delay time  $\tau$  through the correlation function  $M_j(\tau)$  and its derivative  $\dot{M}_j(\tau)$ . This term is a sum of contributions from all the optically active modes of the chromophore and the solvent modes as well. Note, however, that even at this level of approximation, the contributions of the various modes are not additive since the coefficients  $A_j$  and  $B_j$  of the  $j$ th mode depend on all the other modes through  $J_e(t_3; \infty)$  in Eqs. (6.8). For optically dark modes in which  $d_j \approx 0$ , we have  $A_j \approx B_j \approx 0$ . Therefore optically dark modes will not show up in the beats pattern. In the following we shall consider the effect of the optically active modes as well as the solvation modes on the signal. In the Brownian oscillator model, each optically active mode is characterized by the linear coupling strength  $d_j$ , the coherent oscillation frequency  $\omega_j$ , and the dissipative friction constant  $\gamma_j$ , and its dynamics is characterized by the correlation function  $M_j(\tau)$  and its derivative  $\dot{M}_j(\tau)$ . The strongly overdamped modes (whether solvent or intramolecular) are responsible for spectral diffusion processes. Each SOM is characterized by the temperature  $T$ , the solvent reorganization parameter  $\lambda_j$ , and the correlation function of the solvation coordinate  $M_j(\tau)$ . Let us consider  $M_j(\tau)$  of the Brownian oscillator in the four limiting cases [Eqs. (4.12)].

(i) *Coherent oscillations* [Eq. (4.12a)]. For the high-frequency modes of the chromophore in solution we have  $\gamma_j < \omega_j$ . When  $\gamma_j = 0$ , the oscillator experiences a coherent motion with  $M_j(\tau) = \cos\omega_j\tau$  and  $\dot{M}_j(\tau) = -\omega_j \sin\omega_j\tau$ . Equation (6.8a) then assumes the form

$$S(\Omega_2; \tau) \approx S(\Omega_1, \Omega_2; \infty) + 2|\mu_{eg}|^4 [A_j^2(\Omega_2) + \omega_j^2 B_j^2(\Omega_2)]^{1/2} \times \cos(\omega_j\tau + \phi_j), \quad (6.9a)$$

with the phase

$$\phi_j = \arctan[-\omega_j B_j(\Omega_2)/A_j(\Omega_2)]. \quad (6.9b)$$

If we carry the expansion [Eq. (6.7)] to higher orders  $n=2, 3, \dots$ , we obtain higher overtones of the fundamental frequency. The  $n$ th term will contain  $[M_j(\tau)]^n$ , which contains the  $n$ th harmonic ( $n\omega$ ) frequency component. Since the expansion is in powers of  $f_j(t_3; \tau) - f_j(t_3; \infty)$ , which vanishes as  $t \rightarrow \infty$ , it is clear that the successively higher overtones will contribute only at shorter values of the delay time  $\tau$ . Furthermore, due to a coherent interference, the contribution of the overtone beats vanishes as the detuning  $|\Omega_2 - \omega_{eg}|$  is in-

creased. When  $\gamma_j \neq 0$ , but  $\gamma_j < 2\omega_j$ , we have

$$M_j(\tau) = \exp(-\gamma_j \tau / 2) \left[ \cos \bar{\omega}_j \tau + \frac{\gamma_j}{2\bar{\omega}_j} \sin \bar{\omega}_j \tau \right], \quad (6.10a)$$

$$\dot{M}_j(\tau) = -(\omega_j^2 / \bar{\omega}_j) \exp(-\gamma_j \tau / 2) \sin \bar{\omega}_j \tau, \quad (6.10b)$$

with  $\bar{\omega}_j = [\omega_j^2 - (\gamma_j / 2)^2]^{1/2}$ . The first-order beats signal is a simple damped harmonic oscillation with the frequency  $\bar{\omega}_j$  and damping rate  $\gamma_j / 2$ . The second-order contribution will show beats at  $2\bar{\omega}_j$  with damping of  $\gamma_j$ . Again, the overtone contributions vanish as the delay time  $\tau$  or detuning  $|\Omega_2 - \omega_{eg}|$  are increased.

(ii) *Critically damped oscillations* [Eq. (4.12b)]. When  $\gamma_j / 2 = \omega_j$ , we have

$$M_j(\tau) = \exp(-\gamma_j \tau / 2) (1 + \gamma_j \tau / 2), \quad (6.11a)$$

$$\dot{M}_j(\tau) = -(\gamma_j / 2)^2 \exp(-\gamma_j \tau / 2) \tau. \quad (6.11b)$$

The temporal profile of the impulsive signal has two basic components:  $\exp(-\gamma_j \tau / 2)$  and  $\exp(-\gamma_j \tau / 2) \tau$ . The relative contributions of these two components depend on the observation frequency  $\Omega_2$  and can be determined by the parameters  $A_j(\Omega_2)$  and  $B_j(\Omega_2)$ . The higher-order contributions, such as  $\exp(-n\gamma_j \tau / 2)$  or  $\exp(-n\gamma_j \tau / 2) \tau^n$ , may dominate at short delay time  $\tau$ , and for resonant detection  $\Omega_2 \approx \omega_{eg}$ .

(iii) *Overdamped oscillations* [Eq. (4.12c)]. In this case, the dissipative damping is dominant ( $\gamma_j / 2 > \omega_j$ ), and we have

$$M_j(\tau) = \frac{s_+}{s_+ - s_-} \exp(-s_- \tau) - \frac{s_-}{s_+ - s_-} \exp(-s_+ \tau), \quad (6.12a)$$

$$\dot{M}_j(\tau) = -\frac{s_+ s_-}{s_+ - s_-} [\exp(-s_- \tau) - \exp(-s_+ \tau)], \quad (6.12b)$$

with

$$s_{\pm} = \gamma_j / 2 \pm [(\gamma_j / 2)^2 - \omega_j^2]^{1/2}. \quad (6.12c)$$

It should be noted that the impulsive signal, in this case, reaches a maximum at<sup>23</sup>

$$\tau = \frac{1}{s_+ - s_-} \ln \frac{A_j(\Omega_2) - s_+ B_j(\Omega_2)}{A_j(\Omega_2) - s_- B_j(\Omega_2)}. \quad (6.13)$$

(iv) *Strongly overdamped mode* [Eq. (4.12c)]. We now consider the effect of low-frequency and solvent modes on the impulsive signal. Here the SOM dynamics are characterized by the coordinate  $U_j$  [Eq. (5.1)] which undergoes an overdamped motion:  $\gamma_j(s) \gg \omega_j$  (Sec. V). In the linear solute-solvent coupling model, the solvation coordinate is characterized by the reorganization energy  $\lambda_j$  [Eq. (5.4a)], its variance  $\Delta_j^2 = 2k_B T \lambda_j$ , and its correlation function  $M_j(t)$  [Eq. (5.2)]. In the Markovian limit [or Eq. (5.13)]

$$M_j(t) = \exp(-\Lambda_j t). \quad (6.14)$$

Here  $\Lambda_j \equiv \omega_j^2 / \gamma_j$ . The first term in Eq. (6.5a), for a SOM, is negligibly small compared to the second term. Conse-

quently, the contribution of the  $B$  term in Eq. (6.8a) is negligible. The solvation coordinate affects the impulsive signal via  $\lambda_j$ , which introduces the spectral shift and can be easily seen in the frequency domain, and via  $M_j(\tau)$ , which adds a damped background to the impulsive optical signal at a given observation frequency  $\Omega_2$ . We shall now consider the effect of some characteristic solvent motions on the impulsive signal.

(a) *Spectral diffusion limit*. In this limit (cf. Sec. V A), we neglect the solvation dynamics during the optical transition by using the approximation  $M_j(t) \approx M_j(t=0) = 1$  for  $0 < t < t_3$ . In this case, Eqs. (6.5) assume the form

$$f_j(t_3; \tau) = i 2 \lambda_j M_j(\tau) t_3, \quad (6.15a)$$

$$g_j(t_3) = i \lambda_j t_3 + \frac{1}{2} \Delta_j^2 t_3^2. \quad (6.15b)$$

The probe absorption for this case was discussed earlier following Eq. (5.11).

In the analysis of the underdamped oscillation [case (i)], we have indicated that, due to the coherent interference, the contribution of the overtone beats at  $n\omega_j$  vanishes as the detuning is increased. This is also the case when we add a SOM. However, the detuning is now measured by  $|\Omega_2 - \omega_{eg} + \lambda_j|$  with  $\lambda_j > 0$ , instead of  $|\Omega_2 - \omega_{eg}|$ .

(b) *Inhomogeneous broadening*. This is an extreme case of (a) obtained by setting  $M_j(\tau) = M_j(t_3) = M_j(0) = 1$ . In this case, the mode is completely static and Eqs. (6.15) becomes

$$f_j(t_3; \tau) = i 2 \lambda_j t_3, \quad (6.16a)$$

$$g_j(t_3; \tau) = i \lambda_j t_3 + \frac{1}{2} \Delta_j^2 t_3^2. \quad (6.16b)$$

It contributes to the signal in the frequency domain by a convolution with a Gaussian inhomogeneous distribution function centered at the frequency  $\lambda_j$  and with a width  $\Delta_j$ . However, the inhomogeneous broadening does not affect the temporal profile of the impulsive optical signal.

(c) *Homogeneous broadening*. This is the extreme case opposite to case (b). In the homogeneous broadening limit, the solvent nuclear relaxation is infinitely fast

$$M_j(t) = (2 / \Lambda_j) \delta(t). \quad (6.17)$$

For finite delay times  $\tau$  we have  $M_j(\tau) = 0$  and Eqs. (6.5) assume the form [cf. Eq. (5.14)]

$$f_j(t_3; \tau) = 0, \quad (6.18a)$$

$$g_j(t_3) = i (\lambda_j / \Lambda_j) + \hat{\Gamma}_j t_3. \quad (6.18b)$$

The solvation parameters reduce to two:  $\lambda_j / \Lambda_j$  and  $\hat{\Gamma}_j \equiv (\Delta_j^2 / \Lambda_j)$ . In this limit, the solvation coordinate contributes to the signal in the frequency domain through the convolution of  $\sigma_A$  [Eq. (5.15)] with the hole part, and the convolution of  $\sigma_F$  [Eq. (5.15)] with replacing  $\lambda_j$  by  $-\lambda_j$  with the particle part. Homogeneous broadening, like inhomogeneous broadening, does not affect the temporal profile of the impulsive optical signal.

**B. Non-Condon effects  
in impulsive off-resonance spectroscopy**

Earlier in this section we discussed in detail, within the Condon approximation, the optical signal resulting from an impulsive excitation followed by a narrow-band probe detection. This signal is the same as the differential (dispersed at  $\omega_2$ ) signal obtained using an impulsive probe field. If we integrate this signal over  $\omega_2$  (broadband probe), the signal will become independent on  $\tau$ . The reason is that in the Condon approximation the impulsive window function is equal to the unit operator  $\hat{W}=1$ . The beats come from a coherent oscillation, causing the molecule to emit at different frequencies at different times. If at the detection stage we integrate over all frequencies, we lose the beats.

We shall consider now the probe absorption under impulsive off-resonant impulsive pump without invoking the Condon approximation. The signal is now given by Eqs. (6.1)–(6.3) together with (3.18). In this case we need consider only the ground-state contributions since the excited-state doorway vanishes [Eq. (3.18a)]. It should be noted that the ground-state doorway  $\hat{D}_g$  [Eq. (3.18b)] would also vanish had we invoked the Condon approximation and neglected the dependence of  $\mu$  on nuclear coordinates. In the Condon approximation the signal thus vanishes. Relaxing the Condon approximation, the ground doorway state  $\hat{D}_g$  [Eq. (3.18b)], which is nonzero and different from the equilibrium ground-state density matrix, will evolve in time which results in quantum beats. To demonstrate this result, let us consider the optical signal obtained by an off-resonant impulsive pump followed by a resonant impulsive probe. In this case we may represent the probe pulse by a  $\delta$  function and the absorption signal assumes the form

$$S(\Omega_2; \tau) = J_g(0; \tau) = \text{Tr} \{ i [\mu^2(t)\mu^2 - \mu^2\mu^2(\tau)] \rho_g \} \\ \equiv \langle i [\mu^2(\tau), \mu^2] \rangle, \quad (6.19a)$$

with

$$\mu(\tau) = \exp(iH_g\tau)\mu \exp(-iH_g\tau). \quad (6.19b)$$

Here we made use of Eqs. (3.18). The signal in Eq. (6.19a) is related to the  $\mu^2$  response function of the medium. We shall now expand the electronic transition dipole in the nuclear coordinates,

$$\mu = \mu_{eg} \left[ 1 + \sum_j \alpha_j q_j + \dots \right]. \quad (6.20)$$

$q_j$  is the coordinate of the  $j$ th mode, and  $\alpha_j \ll 1$  is an electron-phonon coupling parameter. To lowest order, the signal [Eq. (6.19a)] can be expressed in terms of the coordinate response function

$$S(\Omega_2; \tau) = 4|\mu_{eg}|^4 \sum_j \alpha_j^2 \langle i [q_j(\tau), q_j] \rangle. \quad (6.21)$$

For the harmonic Brownian oscillator model [Eqs. (4.3) and (4.4)], the coordinate response function is given by

$$\langle i [q_j(\tau), q_j] \rangle = \frac{\frac{1}{2} \langle q_j(\tau)p_j + p_j q_j(\tau) \rangle}{\langle p_j^2 \rangle - \langle p_j \rangle^2} \\ = L^{-1} \left[ \frac{\omega_j}{s^2 + s\gamma_j(s) + \omega_j^2} \right] \\ = -\dot{M}_j(\tau)/\omega_j. \quad (6.22)$$

Here  $M_j(\tau)$  is the normalized  $q_j - q_j$  correlation function [Eq. (4.9b) or (5.2)]. Equations (6.21) and (6.22) can be derived using the phenomenological driven oscillator model proposed by Nelson and co-workers<sup>23,24</sup> to interpret the coherent vibrational motions of phonon in matrix and dye molecules in glass and in solvent environments, as well as the librational motions of these systems. Equation (6.19) represents a response function of the dipole operator squared  $\mu^2$  in the ground electronic state. To lowest order in the expansion [Eq. (6.20)], it maps to a driven oscillator moving in the ground electronic surface. However, in the resonant situation, we should evaluate the excited electronic state dynamics as well. This results in a nonequilibrium correlation function in which the time evolution is controlled by the electronic excited state while the ensemble average is taken using the electronic ground-state density matrix. The present analysis shows that the linearly driven oscillator picture is limited to off-resonant situations.

## VII. DISCUSSION

In this paper we developed a systematic theory for time-resolved pump-probe spectroscopy in condensed phases. The doorway-window picture presented in Sec. II allows the rigorous interpretation of these experiments in terms of three stages, involving a preparation, propagation, and detection. The present formalism allows a practical calculation of the time-resolved probe absorption spectrum of polyatomic molecules in condensed phases. In Sec. III we considered some limiting cases, in which the phases of the external fields are not important and the probe signal can be expressed in terms of a convolution of the *bare spectrum* with the (spectral or temporal) intensity profiles of the fields. The calculation of the bare spectrum of the multimode Brownian oscillator molecular model can then be performed using the *Wigner representation* and is carried out in Secs. IV and V. The calculation becomes particularly simple in the impulsive limit where the spectrum may be represented as a single Fourier transform. This case was considered in Sec. VI. The present formalism may be easily applied to optical pulses with arbitrary time scales in which the phases of the fields may also be important. For this purpose we shall divide the total nuclear modes of the system into two groups. The first group contains a small number of relevant modes, which are optically active and their dynamics are fast or comparable to the pulse durations. We shall represent these fast active modes in terms of their vibronic levels with  $|b\rangle, |d\rangle, \dots$ , being the vibronic levels of the electronic excited state manifold and  $|a\rangle, |c\rangle, \dots$ , being the vibronic levels of the ground electronic manifold (Fig. 2). The second group contains

the remaining slow modes. We shall describe these modes in the Wigner phase space representation [Eq. (4.1)], where  $\mathbf{q}$  and  $\mathbf{p}$  are vectors representing the coordinates and the conjugate momenta of the slow modes. The slow modes may include collective solvent motions, rotations, intermolecular librations, or low-frequency intramolecular vibrations. For the slow modes the pulses are assumed to be impulsive and we may invoke Eq. (3.1) for time periods shorter than pulse durations. In this mixed (state and Wigner) representation, Eqs. (2.9)–(2.11)

become

$$S(\Omega_1, \Omega_2; \tau) = \sum_{b,d} \int \int d\mathbf{p} d\mathbf{q} W_{db}^*(\Omega_2; \mathbf{p}, \mathbf{q}) D_{db}(\Omega_1, \tau; \mathbf{p}, \mathbf{q}) \\ + \sum_{c,a} \int \int d\mathbf{p} d\mathbf{q} W_{ca}^*(\Omega_2; \mathbf{p}, \mathbf{q}) \\ \times D_{ca}(\Omega_1, \tau; \mathbf{p}, \mathbf{q}) . \quad (7.1)$$

Here

$$D_{db}(\Omega_1, \tau; \mathbf{p}, \mathbf{q}) = \exp(-i\omega_{db}\tau - \gamma_{db}\tau) \int_{-\infty}^{\infty} d\omega_1 \sum_a P(a) \mu_{da} \mu_{ab} [\hat{E}_1^*(\omega_1) \hat{E}_1(\omega_1 + \omega_{db}) F_e(\omega_1 - \omega_{ba}, \tau; \mathbf{p}, \mathbf{q}) \\ + \hat{E}_1(\omega_1) \hat{E}_1^*(\omega_1 + \omega_{bd}) F_e^*(\omega_1 - \omega_{da}, \tau; \mathbf{p}, \mathbf{q})] , \quad (7.2a)$$

$$D_{ca}(\Omega_1, \tau; \mathbf{p}, \mathbf{q}) = \exp(-i\omega_{ca}\tau - \gamma_{ca}\tau) \int_{-\infty}^{\infty} d\omega_1 \sum_d \mu_{cd} \mu_{da} [P(a) \hat{E}_1^*(\omega_1) \hat{E}_1(\omega_1 + \omega_{ca}) F_g(\omega_1 - \omega_{dc}, \tau; \mathbf{p}, \mathbf{q}) \\ + P(c) \hat{E}_1(\omega_1) \hat{E}_1^*(\omega_1 + \omega_{ac}) F_g^*(\omega_1 - \omega_{da}, \tau; \mathbf{p}, \mathbf{q})] , \quad (7.2b)$$

$$W_{db}(\Omega_2; \mathbf{p}, \mathbf{q}) = \int_{-\infty}^{\infty} d\omega_2 \sum_c \mu_{dc} \mu_{cb} [\hat{E}_2^*(\omega_2) \hat{E}_2(\omega_2 + \omega_{db}) G_e(\omega_2 - \omega_{bc}; \mathbf{p}, \mathbf{q}) + \hat{E}_2(\omega_2) \hat{E}_2^*(\omega_2 + \omega_{bd}) G_e^*(\omega_2 - \omega_{dc}; \mathbf{p}, \mathbf{q})] , \quad (7.3a)$$

$$W_{ca}(\Omega_2; \mathbf{p}, \mathbf{q}) = \int_{-\infty}^{\infty} d\omega_2 \sum_b \mu_{cb} \mu_{ba} [\hat{E}_2^*(\omega_2) \hat{E}_2(\omega_2 + \omega_{ca}) G_g(\omega_2 - \omega_{bc}; \mathbf{p}, \mathbf{q}) + \hat{E}_2(\omega_2) \hat{E}_2^*(\omega_2 + \omega_{ac}) G_g^*(\omega_2 - \omega_{ba}; \mathbf{p}, \mathbf{q})] , \quad (7.3b)$$

with

$$F_m(\omega'_1, \tau; \mathbf{p}, \mathbf{q}) = \int_0^{\infty} dt_1 \exp(i\omega'_1 t_1) \prod_j F_{mj}(t_1, \tau; \mathbf{p}_j, \mathbf{q}_j) , \quad (7.4a)$$

$$G_m(\omega'_2; \mathbf{p}, \mathbf{q}) = \int_0^{\infty} dt_2 \exp(i\omega'_2 t_2) \prod_j G_{mj}(t_2, \tau; \mathbf{p}_j, \mathbf{q}_j) , \\ m = g, e . \quad (7.4b)$$

Here  $F_{mj}$  and  $G_{mj}$  are given by Eq. (4.6). Equations (7.1)–(7.3) provide a unified expression for the pump-probe signal of polyatomic molecules in condensed phases and are valid for arbitrary temporal profiles and durations of the pump and the probe pulses.

Equations (7.2) and (7.3) show explicitly the spectral selectivity induced by the laser pulses. The pump profile  $\hat{E}_1(\omega_1)$  selects vibronic transitions in the doorway functions [Eqs. (7.2)], whereas the probe profile  $\hat{E}_2(\omega_2)$  selects the relevant vibronic transitions for the window functions [Eqs. (7.3)]. In the absence of fast modes (i.e., the pulses are short compared to the nuclear dynamics) we can exclusively use the Wigner representation and Eq. (7.1) reduces to (3.13). In this case, the phases of the laser fields are not important and the signal depends only on their intensities. When the pulse durations are comparable to the nuclear dynamics time scales, the phases of the external fields may become relevant. In addition, the excitation processes may involve only a few (e.g., two) vibronic levels in electronic  $|e\rangle$  manifold and a few in  $|g\rangle$

manifold. In this case the present formalism recovers the theory of vibrational quantum beats obtained by using simplified molecular models with a few vibronic levels.<sup>13,26,27</sup> Furthermore, when the spectral density of the resonant pump field is narrow compared with the vibronic level spacings, the optical selectivity in the doorway functions [Eqs. (7.2)] leads to the selection of  $d=b$  and  $c=a$ . Equation (7.1) then recovers our earlier hole burning results.<sup>15,36</sup> In this case, only the diffusive solvation dynamics as well as the vibronic populations of the chromophore are probed. Vibronic coherences are not created, and the pump-probe signal shows progressions of the chromophore vibronic levels. As the probe delay time  $\tau$  is increased, the holes acquire a time-dependent additional width over the pure homogeneous broadening and the resulting line shape splits into two components [cf. Eq. (3.12) and the following discussion]. The present theory can be easily extended to other related experiments. An application to pump-probe femtosecond spectroscopy of molecular photodissociation has been made recently.<sup>40</sup> The differential signal  $S'$  [Eq. (2.4b)] can be obtained by simply eliminating the  $\omega_2$  integration in Eqs. (7.3). The impulsive stimulated Raman scattering signal measured by Nelson, Ippen, and co-workers<sup>3-10,23,24</sup> is related to  $|P^{(3)}(\mathbf{k}_2, t)|^2$ , which is the same third-order nonlinear polarization [Eq. (A1)] evaluated in this paper. Recently, a sequence of femtosecond pump pulses was used<sup>22</sup> to impulsively pump the optical medium. These experiments

can also be described by the present theory. Their enhanced mode selectivity can be simply attributed to a spectral filtering by the pulses as given by Eqs. (7.1)–(7.4). The optical transmission correlation signal,<sup>11,12</sup> obtained by measuring the transmittance of both the pump field and the probe field, is related to  $P^{(3)}(\mathbf{k}_1, t)$  as well as  $P^{(3)}(\mathbf{k}_2, t)$ . The signal, in this case, is symmetric around  $\tau=0$ . For large delay times  $\tau$ , the transmittance correlation signal is essentially the same as the probe absorption signal considered in this paper. However, for small  $\tau$  in which the pump and probe overlap, we should also include the last four terms in Eq. (A1) to take the coherent artifact into account. Finally, the present formalism may be also used to calculate the time-resolved fluorescence measurement<sup>21,36</sup> where only the excited particle dynamics are probed.

---


$$P^{(3)}(k_2, t)$$

$$\begin{aligned}
&= \int_0^\infty dt_3 \int_0^\infty dt_2 \int_0^\infty dt_1 S^{(3)}(t_3, t_2, t_1) \\
&\quad \times \{ E_2(t-t_3) E_1^*(t+\tau-t_3-t_2) E_1(t+\tau-t_3-t_2-t_1) \exp(i\Omega_2 t_3 + i\Omega_1 t_1) \\
&\quad + E_2(t-t_3) E_1(t+\tau-t_3-t_2) E_1^*(t+\tau-t_3-t_2-t_1) \exp(i\Omega_2 t_3 - i\Omega_1 t_1) \\
&\quad + E_1(t+\tau-t_3) E_2(t-t_3-t_2) E_1^*(t+\tau-t_3-t_2-t_1) \\
&\quad \quad \times \exp[i\Omega_2 t_3 + i(\Omega_2 - \Omega_1)t_2 - i\Omega_1 t_1] \\
&\quad + E_1(t+\tau-t_3) E_1^*(t+\tau-t_3-t_2) E_2(t-t_3-t_2-t_1) \\
&\quad \quad \times \exp[i\Omega_2 t_3 + i(\Omega_2 - \Omega_1)t_1 + i\Omega_2 t_1] \\
&\quad + E_1^*(t+\tau-t_3) E_2(t-t_3-t_2) E_1(t+\tau-t_3-t_2-t_1) \\
&\quad \quad \times \exp[i\Omega_2 t_3 + i(\Omega_2 + \Omega_1)t_2 + i\Omega_1 t_1] \\
&\quad + E_1^*(t+\tau-t_3) E_1(t+\tau-t_3-t_2) E_2(t-t_3-t_2-t_1) \\
&\quad \quad \times \exp[i\Omega_2 t_3 + i(\Omega_2 + \Omega_1)t_2 + i\Omega_2 t_1] \} . \tag{A1}
\end{aligned}$$

Here we have only considered contributions to  $\hat{P}^{(3)}(\omega_2)$  which are second order in pump field and first order in probe. There are, of course, additional third-order terms which are zeroth order in pump and third order in probe which contribute to the  $\omega_2$  Fourier component of the polarization. Those terms, however, represent the saturation of the probe and will not contribute to the difference signal which will be calculated here. The key quantity in the calculation of Eq. (A1) is the nonlinear response function  $S^{(3)}$ , which contains the complete microscopic information necessary for any  $\chi^{(3)}$  measurement, such as four-wave-mixing spectroscopy. In order to simplify the notation, we shall, in the following, introduce the double bracket (Liouville space) notation, in which an ordinary dynamical variable (Hilbert operator)  $A$  is denoted as  $|A\rangle\rangle$ , and the inner product is defined by

$$\langle\langle B|A\rangle\rangle \equiv \text{Tr}(B^\dagger A) . \tag{A2}$$

Using this notation, the nonlinear response function as-

## ACKNOWLEDGMENTS

The support of the National Science Foundation, the Air Force Office of Scientific Research, and the Petroleum Research Fund, administered by the American Chemical Society, is gratefully acknowledged. One of us (S.M.) acknowledges support from the Camille and Henry Dreyfus Foundation.

## APPENDIX A: DOORWAY-WINDOW PICTURE OF PUMP-PROBE SPECTROSCOPY— DERIVATION OF EQ. (2.10)

We start with Eq. (2.4a) by defining the third-order polarization, which is the key quantity in the calculation of the nonlinear spectral signals, and its formal expression is given by<sup>28</sup>

---

sumes the form

$$S^{(3)}(t_3, t_2, t_1) = i^3 \langle\langle V | \mathcal{G}(t_3) \mathcal{V} \mathcal{G}(t_2) \mathcal{V} \mathcal{G}(t_1) \mathcal{V} | \rho(-\infty) \rangle\rangle . \tag{A3}$$

Here  $\mathcal{G}(t)$  is the time evolution operator (Green's function) in the Liouville space in the absence of the external field.  $\mathcal{V}$  is the Liouville space dipole operator. They are defined by their actions on an arbitrary dynamical variable  $A$  (from the left),

$$\mathcal{G}(t)A \equiv \exp(-iHt)A \exp(iHt) , \tag{A4a}$$

$$\mathcal{V}A \equiv VA - AV . \tag{A4b}$$

or (from the right)

$$A\mathcal{G}(t) \equiv \exp(iHt)A \exp(-iHt) , \tag{A4c}$$

$$A\mathcal{V} \equiv AV - VA . \tag{A4d}$$

Physically,  $S^{(3)}$  [Eq. (A3)] gives the polarization response to three  $\delta$  function laser pulses. The time arguments  $t_1$ ,  $t_2$ , and  $t_3$  represent the *time intervals* between successive interactions with the laser fields (see Fig. 1).

The six terms in Eq. (A1) correspond to the  $3! = 6$  permutations representing the different ordering the excitation pulses interacting with the optical medium. It should be noted that in the first two terms of Eq. (A1) the probe field acts after the interactions with the pump field. This ordering of "pump first and probe second" is not

preserved in the last four terms of Eq. (A1). In the remainder of this paper, we shall focus only on processes in which the delayed probe pulse is very well separated from the pump pulse. The system, in this case, is forced to interact first with the pump, and then with the probe. This assumption allows us to neglect the last four terms of Eq. (A1), which contribute to the "coherent artifact" characterizing the experimental signal for delay time shorter than or comparable to the pulse durations.<sup>31</sup> The signal [Eq. (2.4a)], in this case, reduces to

$$\begin{aligned}
 S(\Omega_1, \Omega_2; \tau) = & 2 \operatorname{Re} \int_{-\infty}^{\infty} dt \int_0^{\infty} dt_3 \int_0^{\infty} dt_2 \int_0^{\infty} dt_1 [E_2^*(t+t_3)E_2(t)E_1^*(t+\tau-t_2)E_1(t+\tau-t_2-t_1) \\
 & \times \exp(i\Omega_3 t_3 + i\Omega_1 t_1) \\
 & + E_2^*(t+t_3)E_2(t)E_1(t+\tau-t_2)E_1^*(t+\tau-t_2-t_1) \\
 & \times \exp(i\Omega_3 t_3 - i\Omega_1 t_1)] \\
 & \times \langle\langle V | \mathcal{G}(t_3) \mathcal{V} \mathcal{G}(t_2) \mathcal{V} \mathcal{G}(t_1) \mathcal{V} | \rho(-\infty) \rangle\rangle . \quad (\text{A5})
 \end{aligned}$$

In deriving Eq. (A5), we have changed the integration variable  $t$  to  $t+t_3$ . When the pump and the probe pulses are well separated, we may view a pump-probe experiment as a three-step process: preparation, propagation, and detection. The pump pulse prepares an initial doorway state, which then propagates, and is finally probed at the delay time  $\tau$ . This is the doorway-window picture used in this paper. In order to define the three-step process precisely, let us rewrite Eq. (A5) by changing the integration variable with  $t' = t + \tau - t_2$ . We obtain

$$\begin{aligned}
 S(\Omega_1, \Omega_2; \tau) = & 2 \operatorname{Re} \int_{-\infty}^{\infty} dt \int_0^{\infty} dt_3 \int_{-\infty}^{\tau+t} dt' \int_0^{\infty} dt_1 [E_2^*(t+t_3)E_2(t)E_1^*(t')E_1(t'-t_1) \exp(i\Omega_3 t_3 + i\Omega_1 t_1) \\
 & + E_2^*(t+t_3)E_2(t)E_1(t')E_1^*(t'-t_1) \exp(i\Omega_3 t_3 - i\Omega_1 t_1)] \\
 & \times \langle\langle V | \mathcal{G}(t_3) \mathcal{V} \mathcal{G}(t) \mathcal{G}(t') \mathcal{G}(-t') \mathcal{V} \mathcal{G}(t_1) \mathcal{V} | \rho(-\infty) \rangle\rangle . \quad (\text{A6})
 \end{aligned}$$

Here we have used the identity  $\mathcal{G}(t_2) = \mathcal{G}(t) \mathcal{G}(\tau) \mathcal{G}(-t')$ . When the delay time  $\tau$  is larger than the pulse durations [Eq. (2.9)], we may replace  $\tau+t$  in the upper limit of integration of  $t'$  by  $\infty$ . In this case, the signal reduces to

$$S(\Omega_1, \Omega_2; \tau) = \langle\langle \hat{W}(\Omega_2) | \mathcal{G}(\tau) | \hat{D}(\Omega_1) \rangle\rangle , \quad (\text{A7a})$$

with

$$|\hat{D}(\Omega_1)\rangle\rangle = \int_{-\infty}^{\infty} dt' \int_0^{\infty} dt_1 E_1^*(t') E_1(t'-t_1) \exp(i\Omega_1 t_1) [\mathcal{G}(-t') \mathcal{V} \mathcal{G}(t_1) \mathcal{V} | \rho(-\infty) \rangle\rangle] + \text{H.c.} , \quad (\text{A7b})$$

$$\langle\langle \hat{W}(\Omega_2) | = \int_{-\infty}^{\infty} dt \int_0^{\infty} dt_3 E_2^*(t+t_3) E_2(t) \exp(i\Omega_2 t_3) [\langle\langle V | \mathcal{G}(t_3) \mathcal{V} \mathcal{G}(t) \rangle\rangle] + \text{H.c.} \quad (\text{A7c})$$

Here  $\hat{D}$  is the doorway operator and defines the state prepared by the pump field,  $\hat{W}$  is the window operator defines the detection by the probe field. The time evolution of the system is described by  $\mathcal{G}(\tau)$ . Equations (2.10)–(2.12) can now be obtained by applying Eq. (A7) to the two-level molecular model [Eq. (2.6)] and invoking the rotating-wave approximation.

<sup>1</sup>R. L. Fork, B. I. Greene, and C. V. Shank, *Appl. Phys. Lett.* **38**, 671 (1981); R. L. Fork, C. H. Brito-Cruz, P. C. Becker, and V. C. Shank, *Opt. Lett.* **12**, 483 (1987).

<sup>2</sup>R. J. D. Miller, R. Casalegno, K. A. Nelson, and M. D. Fayer, *Chem. Phys.* **72**, 371 (1982); K. A. Nelson, R. J. D. Miller, D. R. Lutz, and M. D. Fayer, *J. Appl. Phys.* **53**, 1144 (1982).

<sup>3</sup>S. Ruhman, A. G. Joly, and K. A. Nelson, *J. Chem. Phys.* **86**, 6563 (1987).

<sup>4</sup>S. Ruhman, L. R. Williams, A. G. Joly, B. Kohler, and K. A. Nelson, *J. Phys. Chem.* **91**, 2237 (1987).

<sup>5</sup>R. Leonhardt, W. Holzappel, W. Zinth, and W. Kaiser, *Chem.*

*Phys. Lett.* **133**, 373 (1987); A. Laubereau and W. Kaiser, *Rev. Mod. Phys.* **50**, 607 (1978); W. Zinth, M. C. Nuss, and W. Kaiser, *Phys. Rev. A* **30**, 1139 (1984).

<sup>6</sup>C. Kalpouzos, D. McMorrow, W. T. Lotshaw, and G. A. Kenney-Wallace, *Chem. Phys. Lett.* **155**, 240 (1989); **150**, 138 (1988); D. McMorrow, W. T. Lotshaw, and G. A. Kenney-Wallace, *IEEE J. Quantum Electron.* **QE-24**, 443 (1988).

<sup>7</sup>M. M. Robinson, Y. X. Yan, E. B. Gamble, Jr., L. R. Williams, J. S. Meth, and K. A. Nelson, *Chem. Phys. Lett.* **112**, 491 (1984).

<sup>8</sup>S. De Silvestri, J. G. Fujimoto, E. P. Ippen, E. B. Gamble, Jr.,

- L. R. Williams, and K. A. Nelson, *Chem. Phys. Lett.* **116**, 146 (1985).
- <sup>9</sup>L. R. Williams and K. A. Nelson, *J. Chem. Phys.* **87**, 7346 (1987).
- <sup>10</sup>A. M. Weiner, S. DeSilvestri, and E. P. Ippen, *J. Opt. Soc. Am. B* **2**, 654 (1985); A. M. Weiner and E. P. Ippen, *Chem. Phys. Lett.* **114**, 456 (1985).
- <sup>11</sup>M. J. Rosker, F. W. Wise, and C. L. Tang, *Phys. Rev. Lett.* **57**, 321 (1986); F. W. Wise, M. J. Rosker, and C. L. Tang, *J. Chem. Phys.* **86**, 2827 (1987).
- <sup>12</sup>I. A. Walmsley, F. W. Wise, and C. L. Tang, *Chem. Phys. Lett.* **154**, 315 (1989).
- <sup>13</sup>J. Chesnoy and A. Mokhtari, *Phys. Rev. A* **38**, 3566 (1988); A. Mokhtari and J. Chesnoy, *Europhys. Lett.* **5**, 523 (1988).
- <sup>14</sup>P. C. Becker, H. L. Fragnito, J. Y. Bigot, C. H. Brito-Cruz, R. L. Fork, and C. V. Shank, *Phys. Rev. Lett.* **63**, 505 (1989); P. C. Becker, R. L. Fork, C. H. Brito-Cruz, J. P. Gordon, and C. V. Shank, *ibid.* **60**, 2462 (1988).
- <sup>15</sup>C. H. Brito-Cruz, R. L. Fork, W. H. Knox, and C. V. Shank, *Chem. Phys. Lett.* **132**, 341 (1986).
- <sup>16</sup>H. L. Fragnito, J. Y. Bigot, P. C. Becker, and C. V. Shank, *Chem. Phys. Lett.* **160**, 101 (1989).
- <sup>17</sup>S. Saikan, *Phys. Rev. A* **38**, 4669 (1988); S. Saikan, T. Nakabayashi, Y. Kanematsu, and A. Imaoka, *J. Chem. Phys.* **89**, 4609 (1980); Y. Kanematsu, R. Shiraishi, S. Saikan, and T. Kushida, *Chem. Phys. Lett.* **147**, 53 (1988).
- <sup>18</sup>W. R. Lambert, P. M. Felker, and A. M. Zewail, *J. Chem. Phys.* **75**, 5958 (1981).
- <sup>19</sup>J. Chaiken, M. Gurnick, and J. D. McDonald, *J. Chem. Phys.* **74**, 106 (1981).
- <sup>20</sup>See, e.g., S. Haroche, *Am. Phys.* **6**, 189 (1971).
- <sup>21</sup>A. Mokhtari, J. Chesnoy, and A. Laubereau, *Chem. Phys. Lett.* **155**, 593 (1989).
- <sup>22</sup>A. M. Weiner, D. E. Leaird, G. P. Wiederrecht, and K. A. Nelson, *Science* **247**, 1317 (1990); A. M. Wiener, J. P. Heritage, and E. M. Kirschner, *JOSA B* **5**, 1563 (1988).
- <sup>23</sup>Y. X. Yan and K. A. Nelson, *J. Chem. Phys.* **87**, 6240 (1987); **87**, 6257 (1987); Y. X. Yan, L. T. Cheng, and K. A. Nelson, *Advances in Nonlinear Spectroscopy*, edited by R. J. H. Clark and R. E. Hester (Wiley, New York, 1988), p. 299.
- <sup>24</sup>K. A. Nelson and E. P. Ippen, *Adv. Chem. Phys.* **75**, 1 (1989).
- <sup>25</sup>G. Stock and W. Domeke, *Chem. Phys.* **124**, 227 (1988); G. Stock, R. Schneider and W. Domeke, *J. Chem. Phys.* **90**, 7184 (1989).
- <sup>26</sup>M. Mitsunaga and C. L. Tang, *Phys. Rev. A* **35**, 1720 (1987); I. A. Walmsley, M. Mitsunaga, and C. L. Tang, *ibid.* **38**, 4681 (1988).
- <sup>27</sup>A. M. Walsh and R. F. Loring, *Chem. Phys. Lett.* **160**, 299 (1989).
- <sup>28</sup>(a) S. Mukamel, *Phys. Rep.* **93**, 1 (1982); (b) *Adv. Chem. Phys.* **70**, 165 (1988); (c) S. Mukamel and R. F. Loring, *J. Opt. Soc. Am. B* **3**, 595 (1986); (d) Y. J. Yan and S. Mukamel, *J. Chem. Phys.* **86**, 6085 (1987).
- <sup>29</sup>Y. J. Yan and S. Mukamel, *J. Chem. Phys.* **88**, 5735 (1988).
- <sup>30</sup>Y. J. Yan and S. Mukamel, *J. Chem. Phys.* **89**, 5160 (1988).
- <sup>31</sup>R. W. Boyd and S. Mukamel, *Phys. Rev. A* **29**, 1973 (1984).
- <sup>32</sup>B. Bagchi, D. W. Oxtoby, and G. R. Fleming, *Chem. Phys.* **86**, 257 (1984); M. Maroncelli, and G. R. Fleming, *J. Chem. Phys.* **89**, 875 (1988); **86**, 6221 (1987).
- <sup>33</sup>G. van der Zwan and J. T. Hynes, *J. Phys. Chem.* **89**, 4181 (1985).
- <sup>34</sup>S. Kinoshita, N. Nishi, and T. Kushida, *Chem. Phys. Lett.* **124**, 605 (1987).
- <sup>35</sup>P. F. Barbara and W. Jarzeka, *Acc. Chem. Res.* **21**, 195 (1988).
- <sup>36</sup>R. F. Loring, Y. J. Yan, and S. Mukamel, *J. Chem. Phys.* **87**, 5840 (1987); *J. Phys. Chem.* **91**, 1302 (1987).
- <sup>37</sup>W. B. Bosma, Y. J. Yan, and S. Mukamel (unpublished).
- <sup>38</sup>M. Dantus, M. J. Rosker, and A. H. Zewail, *J. Chem. Phys.* **87**, 2395 (1987); T. S. Rose, M. J. Rosker, and A. H. Zewail, *ibid.* **88**, 6672 (1988).
- <sup>39</sup>M. Dantus, R. M. Bowman, J. S. Baskin, and A. H. Zewail, *Chem. Phys. Lett.* **159**, 406 (1989).
- <sup>40</sup>Y. J. Yan, L. E. Fried, and S. Mukamel, *J. Phys. Chem.* **93**, 8149 (1989).
- <sup>41</sup>R. Kosloff, S. A. Rice, P. Gaspard, S. Tersigni, and D. J. Tannor, *Chem. Phys.* **139**, 201 (1989).
- <sup>42</sup>Y. R. Shen, *The Principles of Nonlinear Optics* (Wiley, New York, 1984), p. 216.
- <sup>43</sup>M. Lax, *J. Chem. Phys.* **20**, 1752 (1952).
- <sup>44</sup>S. Mukamel and Y. J. Yan, *Acc. Chem. Res.* **22**, 301 (1989).
- <sup>45</sup>M. Hillery, R. F. O'Connell, M. O. Scully, and E. P. Wigner, *Phys. Rep.* **106**, 121 (1984).
- <sup>46</sup>H. Mori, I. Oppenheim, and J. Ross, in *Studies in Statistical Mechanics*, edited by J. deBoer and G. E. Uhlenbeck (North-Holland, Amsterdam, 1962), Vol. 1; J. T. Hynes, J. M. Deutch, C. H. Wang, and I. Oppenheim, *J. Chem. Phys.* **48**, 3085 (1968).
- <sup>47</sup>S. A. Adelman, *J. Chem. Phys.* **64**, 124 (1976).
- <sup>48</sup>H. Risken, *The Fokker-Planck Equation* (Springer, Berlin, 1984).
- <sup>49</sup>H. Mori, *Prog. Theor. Phys.* **33**, 423 (1965); M. Tokuyama and H. Mori, *ibid.* **55**, 411 (1976).
- <sup>50</sup>Y. J. Yan and S. Mukamel, *J. Phys. Chem.* **93**, 6991 (1989); Y. J. Yan, M. Sparpaglione, and S. Mukamel, *ibid.* **92**, 4842 (1989).
- <sup>51</sup>R. A. Marcus and N. Sutin, *Biochem. Biophys. Acta* **811**, 275 (1985); H. Sumi and R. A. Marcus, *J. Chem. Phys.* **84**, 4894 (1986).
- <sup>52</sup>R. F. Loring and S. Mukamel, *J. Chem. Phys.* **87**, 1272 (1987).
- <sup>53</sup>L. E. Fried and S. Mukamel (unpublished).
- <sup>54</sup>C. J. F. Böttcher and P. Bordewijk, *Theory of Electronic Polarization* (Elsevier, Amsterdam, 1978), Vol. II.
- <sup>55</sup>N. Bloembergen, E. M. Purcell, and R. V. Pound, *Phys. Rev.* **73**, 679 (1948); P. W. Anderson and P. R. Weiss, *Rev. Mod. Phys.* **25**, 269 (1953); R. Kubo, *Adv. Chem. Phys.* **15**, 101 (1969).